Journal of Medicinal Chemistry

pubs.acs.org/jmc Article

Heparan Sulfate Mimetics Differentially Affect Homologous Chemokines and Attenuate Cancer Development

Chethan D. Shanthamurthy, Shani Leviatan Ben-Arye, Nanjundaswamy Vijendra Kumar, Sharon Yehuda, Ron Amon, Robert J. Woods, Vered Padler-Karavani,* and Raghavendra Kikkeri*

Cite This: J. Med. Chem. 2021, 64, 3367−3380 Read Online

ACCESS | Metrics & More | Article Recommendations | Supporting Information

ABSTRACT: Achieving selective inhibition of chemokine activity by structurally well-defined heparan sulfate (HS) or HS mimetic molecules can provide important insights into their roles in individual physiological and pathological cellular processes. Here, we report a novel tailor-made HS mimetic, which furnishes an exclusive iduronic acid (IdoA) scaffold with different sulfation patterns and oligosaccharide chain lengths as potential ligands to target chemokines. Notably, highly sulfated-IdoA tetrasaccharide (**I-45**) exhibited strong binding to CCL2 chemokine thereby blocking CCL2/CCR2-mediated *in vitro* cancer cell invasion and metastasis. Taken together, IdoA-based HS mimetics offer an alternative HS substrate to generate selective and efficient inhibitors for chemokines and pave the way to a wide range of new therapeutic applications in cancer biology and immunology.

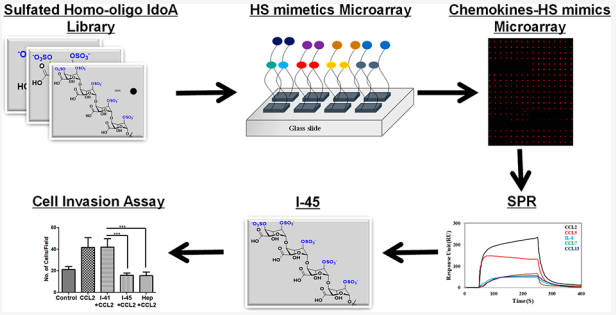

INTRODUCTION

Chemokines are a family of small proteins that have become a focus of extensive research due to their diverse roles in numerous physiological and pathological processes[1−3] including cell trafficking, angiogenesis, embryonic development, neurodegenerative diseases, and cancer.[4−10] Thus, the selective inhibition of chemokines can be beneficial in controlling inflammation, viral entry, and cancer progression.[11,12] Despite two decades of research in this area, only two antagonists for chemokine receptors have successfully passed clinical trials.[13−15] Hence, there is an urgent need for new approaches in controlling chemokine activity. It has been shown that chemokines utilize the highly sulfated glycosaminoglycan (GAG) heparan sulfate (HS) as a co-receptor to oligomerize and activate their cell surface receptors.[16−22] As a result, identifying the core HS structures responsible for specific chemokine activity is an attractive target for medicinal applications.

HS is composed of α(1,4)-linked disaccharide units of D-glucosamine and a hexuronic acid, which can be either D-glucuronic acid (GlcA) or L-iduronic acid (IdoA) with different sulfate modifications.[23−29] Theoretically, HS tetrasaccharides can be arranged into 2304 combinations (48 × 48), highlighting the structural diversity of HS for molecular recognition. The pioneering work of Linhardt, Seeberger, Boons, Hung, Hsieh-Wilson, Desai, Turnbull, Liu, and Gardiner introduced reliable chemical and chemoenzymatic protocols to synthesize HS libraries in order to decipher the sulfation codes and oligosaccharide sequences essential for chemokines and other HS-binding proteins (HSBPs).[30−47] However, it was noted that most chemokines could bind to more than one HS sequence, and the same HS sequence may interact with more than one chemokine or HSBP. Consequently, the discovery of a specific HS structural domain to modulate individual chemokines has been highly challenging.

Alternatively, HS mimetics can be synthesized using the essential structural features of native HS that are responsible for its performance. These features can be incorporated into a simplified chemical structure to modulate specificity in chemokine recognition. A broad range of HS mimetics has been reported in the literature.[48,49] However, these HS mimetics are featureless in terms of conformational plasticity and sulfation patterns, which are key properties of HS used in fine-tuning the binding affinities of HSBPs. Here, we report a new set of tailor-made HS mimetics, which can use their sulfation patterns, conformational plasticity, and oligosaccharide chain length to modulate their binding characteristics to homologous chemokines. Candidates with high affinities to specific chemokines were identified by microarray screening and further utilized in cancer therapy assays.

Received: December 21, 2020
Published: March 8, 2021

https://dx.doi.org/10.1021/acs.jmedchem.0c01800
J. Med. Chem. 2021, 64, 3367−3380

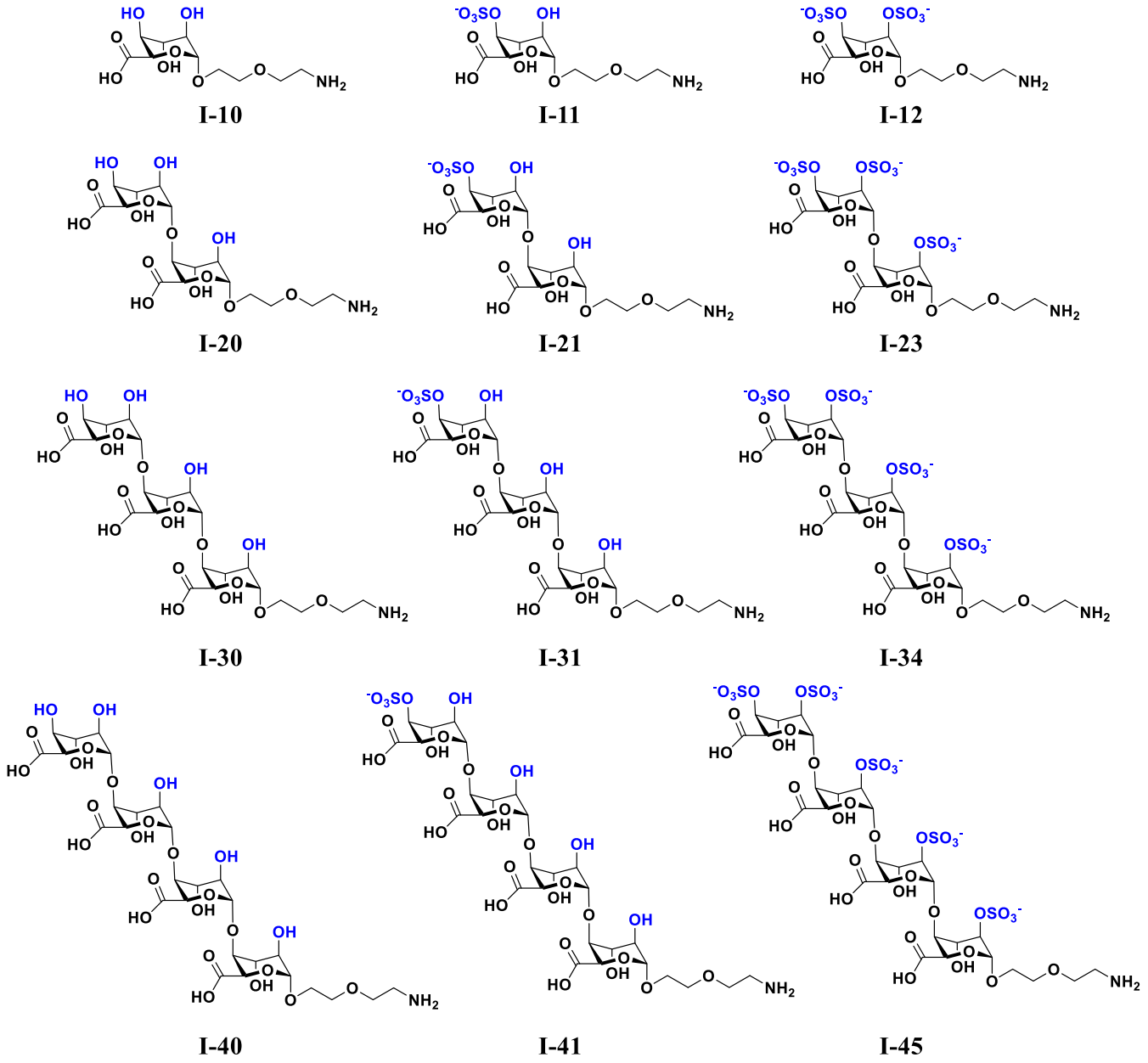

Figure 1. Structures of HS mimetics.

RESULTS AND DISCUSSION

The synthesis of sulfated iduronic acid homo-oligosaccharides (Figure 1) is not straightforward as IdoA is not commercially available and controlling the α-glycosidic linkages between the successive IdoA residue is difficult. We have reported previously a new linear approach to synthesize oligo-IdoA. Our core building blocks 1,6-anhydro-β-L-idopyranosyl 4-alcohol (1) and iduronic acid-thiophenol (2) were synthesized from 1,2:5,6-di-*O*-isopropylidene-α-D-glucofuranose by six- and nine-step reactions, using described procedures,[50] with a total yield of 0.27 and 0.31%, respectively. Using 1 and 2 as acceptor and donor, respectively, successive IdoA residue were installed by five-step linear reactions.[50]

Briefly, 1 and 2 were reacted in the presence of NIS and TMSOTf promotor, followed by acetolysis of the anhydro-ring in the presence of copper(II) trifluoromethanesulfonate [$Cu(OTf)_2$] and acetic anhydride. Then, successive thioglycosylation, mild deacetylation, one-pot TEMPO oxidation, and benzyl esterification yielded the di-IdoA donor. Glycosylation of di-IdoA donor with an azide-linker yielded fully protected di-IdoA intermediate (**L-2**). Similar reaction conditions with di- or tri-IdoA donor (**3** and **4**) and acceptor **1** yielded tri- and tetra-IdoA precursors (**L-3** and **L-4**). Global deprotection of these precursors yielded desired non-sulfate IdoA ligands (I-10, I-20, I-30, and I-40) (Figure 2). For IdoA(4S) ligands (I-11, I-21, I-31, and I-41), IdoA precursors were subjected to selective levulinoyl (Lev) deprotection and sulfation, followed by global deprotection. Highly sulfated-IdoA oligosaccharide series (I-12, I-23, I-34, and I-45) were obtained by de-esterification, followed by sulfation and hydrogenolysis. All final compounds were purified by ion-exchange resin chromatography, followed by a bond elute column. Their structures and purity were confirmed by standard NMR and mass spectrometry techniques.

To identify hidden HS-binding active sites on chemokines, we constructed a microarray platform of HS mimetics. The

https://dx.doi.org/10.1021/acs.jmedchem.0c01800
J. Med. Chem. 2021, 64, 3367−3380

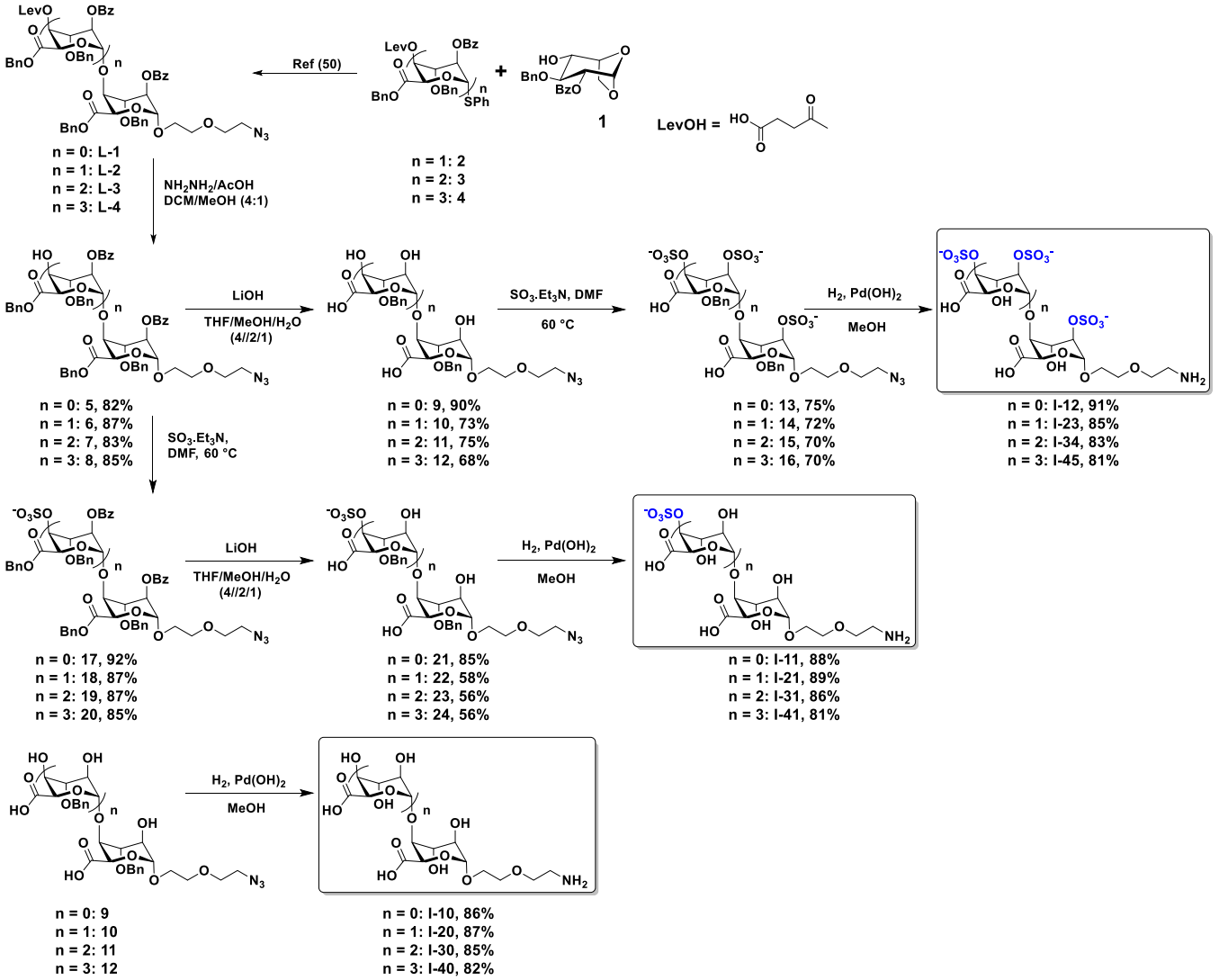

Figure 2. Synthesis of sulfated oligo-IdoA derivatives.

synthetic HS mimetics were printed onto epoxide-functionalized microarray slides in replicates of four, as described in the Experimental Section, and tested on three homeostatic chemokines (CCL28, CXCL12, and CCL12) and six inflammatory chemokines [CXCL8 (IL-8), CXCL10 (IP-10), CCL2 (MCP-1), CCL7 (MCP-3), CCL13 (MCP-4), and CCL5 (RANTES)]. The rationale for selecting these chemokines is based on their structural and functional homologues properties, particularly CCL2, CCL7, and CCL13 share high sequence homology.[51] Identifying active HS ligands for these chemokines is important to monitor their specific activity. To validate the binding order of HS mimetics with chemokines, we ranked each glycan based on percentage of its relative fluorescent intensity against the optimal fluorescent signal.[52,53] Based on the binding patterns, we further divided them into four distinct groups (Figure 3a). In group A, we found that CCL13 (MCP-4), an inflammatory chemokine, and CCL28, a homeostatic chemokine, showed a broad spectrum of moderate and strong binding with HS mimetics, indicating that these two chemokines display promiscuous HS binding sites and reinforced the hypothesis that sulfation group is not a key structure feature for these chemokines' binding. Furthermore, these results suggested that group A chemokines may require native HS synthetic analogues to establish selectivity.

In group B, we found that the homeostatic chemokines CXCL12 and CCL21 displayed weak or moderate binding with non-sulfated IdoA ligands (ranked 38−66% for **I-10** to **I-40**) and strong binding to sulfated HS mimetics (Figure 3a). Both homeostatic chemokines displayed a systematic enhancement in affinity with the increasing length of oligosaccharides (**I-11** to **I-31** ranked 64%, 79%, and 92% with CXCL12 and 62%, 71%, and 83% with CCL21; **I-12** to **I-23** ranked 75% and 98% with CXCL12 and 79% and 86% with CCL21). Surprisingly, they both displayed weak binding with the tetrasaccharide **I-41**, whereas **I-45** had strong binding to CXCL12 (ranked 91%), but not to CCL21. These findings demonstrated that optimal homo-oligosaccharide chain length and sulfation code is critical for molecular-level interaction.

Finally, we compared the binding profile of five inflammatory chemokines, CXCL10 (IP-10), CCL7 (MCP-3), CXCL8 (IL-8), CCL5 (RANTES), and CCL2 (MCP-1) (Figure 3a). Based on their binding patterns, we classified them into groups C and D. In group C, chemokines CXCL10, CCL7, and CXCL8 displayed a strong binding with mono and highly sulfated IdoA analogues and weak binding with non-sulfate

https://dx.doi.org/10.1021/acs.jmedchem.0c01800
J. Med. Chem. 2021, 64, 3367−3380

(a)

Sulfation	ID	Charge			A		B		C			D		%
		Sulfate	Uronate	Net	CCL13	CCL28	CXCL12	CCL21	CXCL10	CCL7	CXCL8	CCL5	CCL2	
None	I-10	0	-1	-1	74	46	62	52	47	30	17	2	4	100
	I-20	0	-2	-2	82	58	66	63	45	30	12	2	2	75
	I-30	0	-3	-3	69	72	38	46	24	17	5	1	0	50
	I-40	0	-4	-4	67	56	56	48	44	33	12	2	2	25
Mono-4-*O*-Sulfate	I-11	-1	-1	-2	81	80	64	62	57	58	62	15	23	0
	I-21	-1	-2	-3	94	84	79	71	67	55	73	38	25	
	I-31	-1	-3	-4	86	80	92	83	78	75	63	30	36	
	I-41	-1	-4	-5	72	54	45	60	23	12	13	10	0	
Di-2,4-*O*-Sulfate	I-12	-2	-1	-3	53	51	75	79	82	94	71	75	66	
	I-23	-3	-2	-5	88	76	98	86	96	87	83	86	69	
	I-34	-4	-3	-7	67	84	82	80	74	79	95	80	67	
	I-45	-5	-4	-9	70	72	91	50	87	80	96	91	88	
Pearson r charge-binding		Sulfate			ns	ns	*	ns	**	**	***	****	****	
		Uronate			ns	ns	ns	ns	ns	ns	ns	ns	ns	
		Net			ns	ns	ns	ns	ns	ns	*	*	*	

(b)

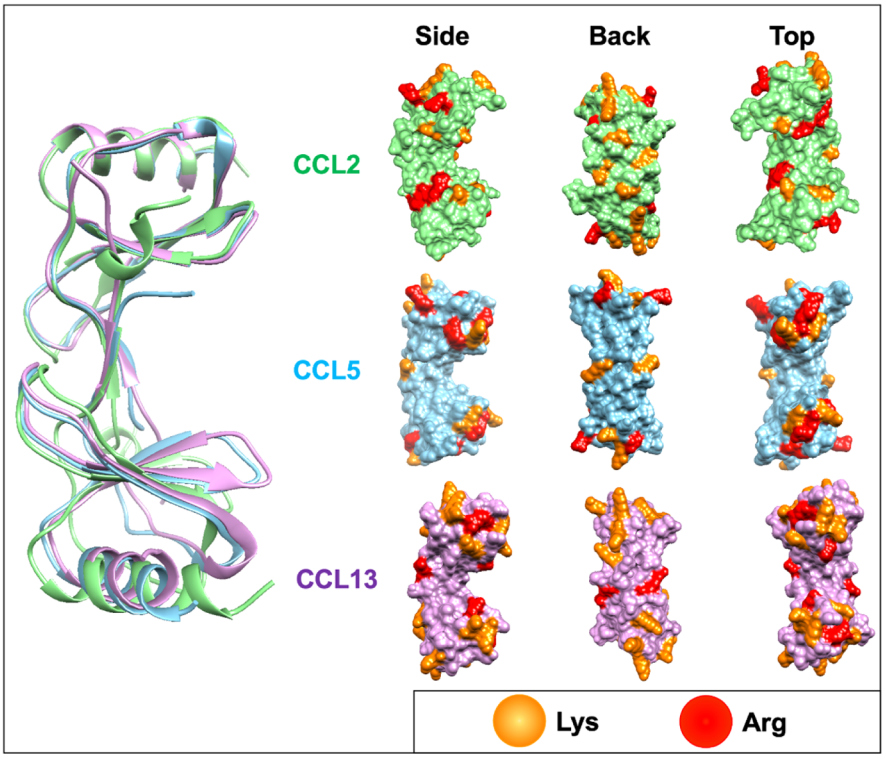

Figure 3. Chemokine glycan microarray binding assay and structural analysis. (a) Binding was tested at three serial dilutions, then detected with the relevant biotinylated secondary antibody (1 μg/mL) followed by Cy3-Strepavidin (1.5 μg/mL) (Figure S3). Arrays were scanned, relative fluorescent units (RFU) obtained for each chemokine, and mean rank between the three dilutions was calculated for glycans printed at 100 μM concentration. For this purpose, the binding RFUs per dilution per glycan was determined, then maximum RFUs in each detection were determined and set as 100% binding and all other glycans were calculated as a ratio of max (percent). The rank for each glycan was averaged between the three dilutions for each detection and SEM was carried out. This analysis allowed to compare the glycans' binding patterns across chemokines. The mean rank is shown as a heatmap of all examined binding assays together (red highest, blue lowest, and white 50th percentile of ranking). Pearson correlation between charge and binding was analyzed (Prism 8) revealing a strong dependance on ligand charge on the binding for CCL2, CCL5, and CXCL8. (b) Structures of CCL2, CCL5, and CCL13 (PDB IDs: 1DOK, 5COY, and 2RA4, respectively) were aligned using the MatchMaker tool in the Chimera modeling package Chimera (UCSF Chimera—a visualization system for exploratory research and analysis)[61] and resulted in average root-mean-square deviation (RMSD) of 1.44 Å. Regions of positive charge (lysine and arginine) were highlighted on the solvent-accessible surfaces and revealed no conspicuous similarities between CCL13 versus CCL5 or CCL2, despite dramatic differences in HS mimetics recognition by the glycan microarrays (a).

IdoA analogues, indicating that sulfate groups are key regulators in inflammatory chemokines. Unlike group C, chemokines CCL5 and CCL2 showed exclusive strong binding to high-sulfated HS mimetics, no binding to non-sulfated mimetics, and weak binding with a mono-sulfated ligand. Among high-sulfate ligands, **I-23** and **I-45** revealed strong binding to group D chemokines, indicating that sulfation code, even number of IdoA units, and absolute $^{1}C_{4}$-IdoA

https://dx.doi.org/10.1021/acs.jmedchem.0c01800
J. Med. Chem. 2021, 64, 3367−3380

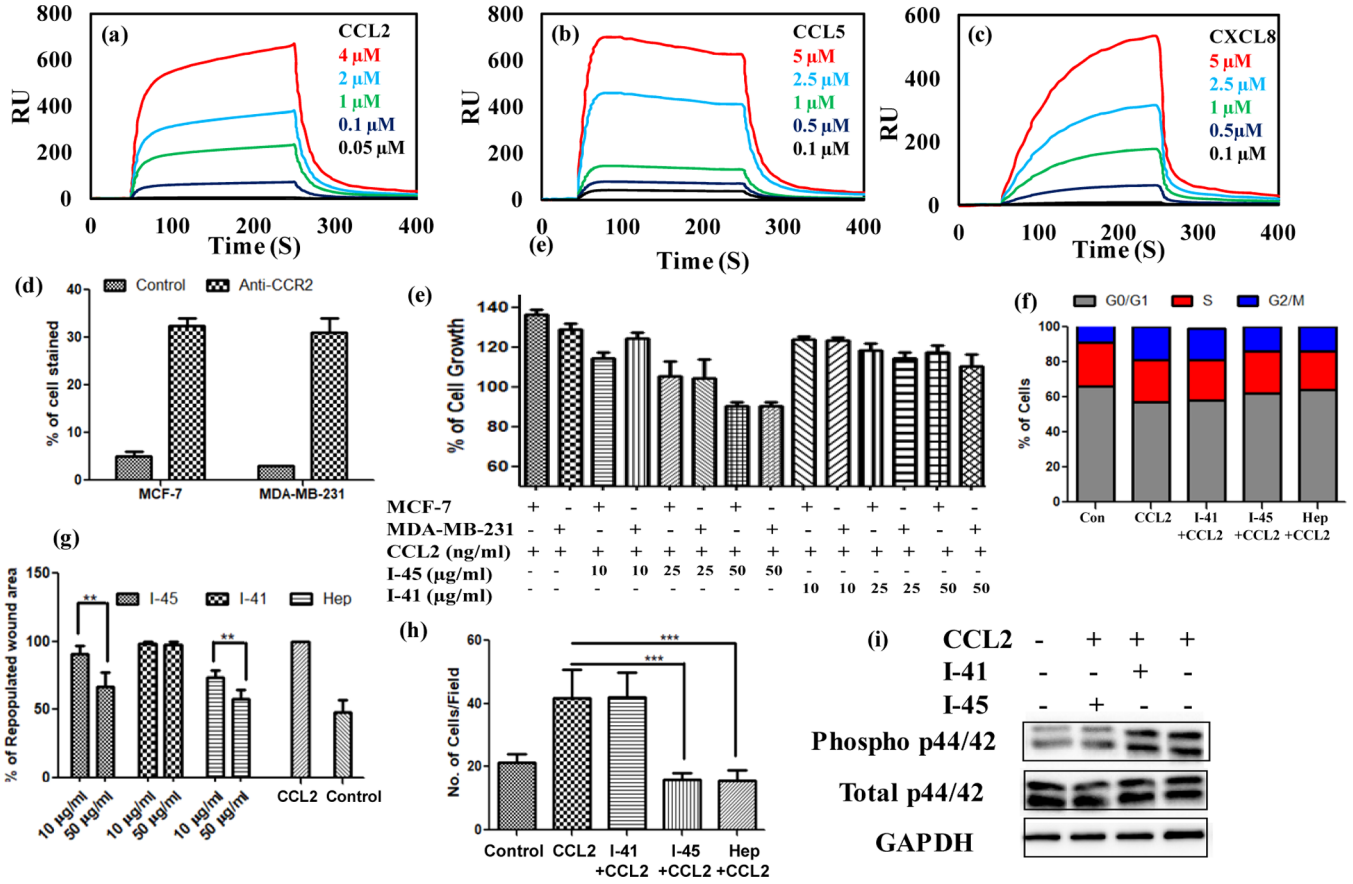

Figure 4. (a) SPR binding analysis of the interaction between CCL2 (0.05−4 μM) and **I-45;** a global fit according to a 1:1 binding model was applied, resulting in dissociation constant (K_D) of 1.67 ± 0.3 μM, k_{on} of 1.26 ± 0.08 × 10^5 M^{-1} s^{-1}, and k_{off} of 2.1 ± 0.5 × 10^{-1} s^{-1}; (b) SPR binding analysis between CCL5 (0.1−5 μM) and **I-45**: (K_D) of 5.72 ± 0.24 μM, k_{on} of 4.2 ± 0.46 × 10^4 M^{-1} s^{-1}, and k_{off} of 2.4 ± 0.38 × 10^{-1} s^{-1}; (c) (K_D) of CXCL8 (0.1−5 μM) with **I-45** is 9.34 ± 0.21 μM, k_{on} of 3.16 ± 0.08 × 10^5 M^{-1} s^{-1}, and k_{off} of 2.96 ± 0.1 × 10^{-1} s^{-1}; (d) FACS quantification of anti-CCR2 expression level by MCF-7 and MDA-MB-231 cell lines; (e) WST assay for MCF-7 and MDA-MB-231 cells proliferation after 48 h treatment of ligand and chemokines. The bar graphs indicated the percentage of cell growth. (f) MCF-7 cell cycle progress in the presence and absence of HS ligands; (g) Wound healing assay: Area repopulated in 5 h. Data expressed as mean ± SD (n = 3; $^{**}P < 0.01$); (h) Inhibition of CCL2-mediated cell migration through matrigel monolayer containing **I-45**, **I-41**, and **Hep** (50 μg/mL) and CCL2 (50 ng). Data expressed as mean ± SD (n = 3; $^{***}P < 0.001$); (i) MAPK pathway analysis: MCF-7 cells were treated with **CCL2** (50 ng/mL) with and without **I-45** and **I-41** ligands (50 μg/mL) and cell lysate after 30 min was quantified for P-p44/42 and total p44/42.

conformation[54] are critical for CCL2 and CCL5 activation. Interestingly, 4-*O*-sulfation enhances the population of the $^1C_4$ geometry, and this conformer becomes exclusive upon additional 2-*O*-sulfation. Overall, the microarray analysis revealed a strong interaction between **I-45** with CCL2, CCL5, CXCL8, CXCL10, and CXCL12 (ranked 88%, 91%, 87%, and 91%).

We then investigated the effect of charge on binding recognition of HS mimetics, considering the charge contribution from the sulfate, uronate, and total net charge. This analysis revealed that the binding for chemokines of groups C and D correlated directly with the net sulfation charge in contrast to the case of chemokines from groups A and B where there was no correlation between ligand charge and binding (Figure 3a). Inclusion of the net charge from the uronic acid moieties further differentiated the binding associated with CCL2, CCL5, and CXCL8 (Figure 3a), while CCL2 and CCL5 seemed to have higher selectivity toward the di-2,4-*O*-sulfate compounds. To generate structure-based insights, we examined available crystal structures of these chemokines. As expected, the structure of CXCL8 was very different from CCL2/5, since CC chemokines are known to have a distinctly different structural motif compared to CXC chemokines.[19,55] Notably, although we observed very strong structural similarities between CCL2, CCL5, and CCL13 (Figure 3b), their binding characteristics differ dramatically. While CCL13 displayed minimal selectivity to HS mimetics, both CCL2 and CCL5 strongly preferred binding to the extensively charged di-2,4-*O*-sulfate compounds (Figure 3a). Considering that binding of GAGs to chemokines is known to be mediated by ionic interactions, we compared the distribution of the positively charged amino acids (lysine and arginine) on the surface of CCL2, CCL5, and CCL13 (Figure 3b). Remarkably, there were no obvious similarities in the distributions of arginine and lysine residues on the surfaces of CCL2, CCL5, or CCCL13. These findings suggest that the interactions between chemokines and the HS mimetics of varying sulfation patterns may be particular to each chemokine and may not stem from a shared binding motif. This conclusion is consistent with previous studies showing that, although the affinity of CCL5 and heparin tetrasaccharides is sensitive to sulfation patterns, the contacts are dynamic and do not favor a single well-defined binding motif.[56] A structural interpretation of the interactions is further complicated by the fact that chemokines can adopt a

https://dx.doi.org/10.1021/acs.jmedchem.0c01800
J. Med. Chem. 2021, 64, 3367−3380

wide range of oligomerization states that play key roles in mediating binding to GAGs[19] and interactions with their receptors.[57]

To quantitatively evaluate the binding affinity between **I-45** and chemokines, SPR experiment was performed using five different chemokines (CCL2, CCL5, CXCL8, CXCL10, and CXCL12), which showed strong selective and sensitive binding in microarray experiments. The equilibrium binding constants (K_D) measured from steady state fit. **I-45** revealed strong binding to CCL2 chemokine (1.6 μM) as compared to other chemokines (CCL5: 5.72 μM; CXCL10: 19.54 μM; CXCL8: 9.34 μM; and CXCL12: 18.78 μM) (Figures 4a–c, S1, and S2), indicating that **I-45** is the ideal ligand to target CCL2 activity. To date, CCL2 is only the second chemokine shown to specifically recognize iduronic acid scaffold. The **I-12** (di-2,4-*O*-sulfated IdoA)-CCL20 chemokine was the first example of the specific interaction mediated by IdoA scaffold.[31]

CCL2 and its CCR2 receptors are highly expressed in several breast cancer cells and play a pivotal role in cancer cell invasion and metastasis.[58,59] Therefore, inhibiting CCL2 signaling offers opportunities for drug discovery to target triple-negative breast cancer (TNBC). Here, we selected MCF-7 and MDA-MB-231 breast cancer cells to target CCR2/CCL2 activity, which is known to express a high level of CCR2 and at the same time, a low level of autocrine CCL2 chemokines, which is the ideal condition to test external CCL2-mediated cellular activity.[58,59] The expression of CCR2 on MCF-7 and MDA-MB-231 was further confirmed by flow cytometry (Figures 4d and S4).

Next, a cancer cell proliferation assay was performed with **I-45** with CCL2. **I-41** and native heparin were used as negative and positive controls, respectively, and cell proliferation was evaluated using water-soluble tetrazolium (WST) assay. Interestingly, the addition of **I-45** to CCL2-treated cells showed ~40–50% reduction in cell proliferation after 48 h (Figure 4e) as compared to **I-41**, confirming that **I-45** is a potential ligand to inhibit the CCL2-mediated cell proliferation. To investigate the mechanism of cell proliferation, we performed cell–division cycle analysis using flow-cytometric analysis of their DNA content (Figure 4f). The cell cycle analysis clearly revealed that most of the cells were in G0/G1 state which changed upon the addition of CCL2 that induced S and G2/M phases. On the other hand, the addition of **I-45** and **Hep** reduced the G2/M phases from 19% and 14%, when compared to **I-41**, indicating that **I-45** displayed a marginal effect on cell proliferation.

Next, we tested whether **I-45** can inhibit CCR2/CCL2-mediated cell migration using wound healing assay (Figure 4g). Cancer cells were grown to a monolayer in 24-well plates and wounds were generated by using the sterile tip. The bright-field images were recorded, quantified, and monitored for several hours.[60] CCL2 (50 ng) induced complete wound closure after 5 h (considered as 100% migration). However, the addition of **I-45** (50 μg/mL) with CCL2 (50 ng) showed 34% reduction in the cell migration, **I-41** had no effect, and natural heparin showed 42% reduction in the cell migration. These results clearly illustrate that **I-45** is a potential small molecule to target CCL2. Finally, we performed cell invasiveness by Boyden chamber assay in the presence of **I-41** and **I-45** (Figures 4h and S5). The results correlate to the cell migration assay, where **I-45** significantly reduces cell invasiveness. To further investigate the invasiveness mechanism, we analyzed the expression level of MAP kinase. Western blot analysis of p42/44 showed that MCF-7 cells treated with **I-45**/CCL2 expressed a low level of MAPK compared to that with CCL2- or **I-41**/CCL2-treated cells (Figures 4i and S6). Overall, these results suggest that **I-45** can be considered as a potential ligand to modulate CCL2 activity and anti-cancer therapy. Unlike the endogenously expressed heparin, these defined chemically-synthesized molecules have better and controllable therapeutic applications.

CONCLUSIONS

In conclusion, we have demonstrated the key role of IdoA scaffold in chemokine interactions and thereby unraveled the unique structural requirement to modulate sequence homologous chemokines. To our knowledge, CCL2 is only the second chemokine currently known in the literature to recognize IdoA scaffolds selectively. These findings lay the foundations for developing IdoA-based drug molecules for cancer and immunotherapy.

EXPERIMENTAL SECTION

General Instructions. All chemicals were reagent grade and used as supplied except where noted. Analytical thin-layer chromatography (TLC) was performed on Merck silica gel 60 F254 plates (0.25 mmol). Compounds were visualized by UV irradiation or dipping the plate in ceric ammonium molybdate (CAM)/ninhydrin solution followed by heating. Column chromatography was carried out using force flow of the indicated solvent on Flukab Kieselgel 60 (230–400 mesh). ^{1}H and ^{13}C NMR spectra were recorded on a Jeol 400 MHz with a cryo probe using residual solvent signals as an internal reference ($CDCl_3$ δ_H, 7.26 ppm, δ_C 77.3 ppm and CD_3OD δ_H 3.31 ppm, δ_C 49.0 ppm). The chemical shifts (δ) are reported in ppm and coupling constants (J) in Hz. The purity of all final compounds (purity above 95%) was confirmed from NMR and mass spectrometry. **I-45** and **I-41** purity was further confirmed by PAMN-HPLC using monopotassium phosphate 1 M for 30 min at a flow rate of 0.5 mL/min.

General Procedure for Lev Deprotection. The compound (**L-1**/**L-2**/**L-3**/**L-4**) was dissolved in a mixture of dry DCM/MeOH (4/1) and 5 equiv of hydrazinehydrate ($H_2NNH_2{\cdot}H_2O$), and acetic acid (for 1 mg, 1 mL) was added, under nitrogen atmosphere. The reaction flask was stirred for another 4 h. After completion of the reaction and quenching with 10 mL of acetone, the solvent was evaporated under reduced pressure. The residue was purified by flash column chromatography (EtOAc/hexane = 1/1) to afford the Lev deprotected compound.

General procedure for ester deprotection. The compound (**5**/**6**/**7**/**8**/**17**/**18**/**19**/**20**) was dissolved in THF/MeOH/$H_2$0 water mixture (4/2/1). 50 equiv. of $LiOH{\cdot}H_2O$ was added. The reaction flask was stirred for 2–3 days. After completion of the reaction and quenching with amberlite IR120 acidic resin (if the compound is sulfated, quench with Dowex 50WX8 H^+ resin), the reaction mixture was filtered and evaporated under reduced pressure and purified using silica column chromatography using DCM and MeOH as eluents to deprotect the compound.

General Procedure for *O*-Sulfation. The compound (**5**/**6**/**7**/**8**/**9**/**10**/**11**/**12**) was dissolved in dry DMF (6 mL). $SO_3{\cdot}Et_3N$ (OH 5 equiv per OH group) was added. The reaction flask was stirred for 3 days at 60 °C. After completion of the reaction, it was cooled to room temperature (RT), aqueous solution of $NaHCO_3$ (10 equiv per OH group) was added and kept for another 16 h. The reaction mixture was filtered using whatman filter paper 41 and washed with DCM/MeOH (1/1, 10 mL); the solvent was evaporated under reduced pressure and the resulting residue was purified using a silica column chromatography (DCM/MeOH = 1/9 for mono sulfated compound). For highly sulfated analogues, the compound was purified by using Sephadex LH-20 resin and eluted with 50% DCM, MeOH, and passed through a sodium (Na^+) resin column using water as an eluent.

https://dx.doi.org/10.1021/acs.jmedchem.0c01800
J. Med. Chem. 2021, 64, 3367–3380

The product fraction was lyophilized to afford sulfated compounds as a white powder.

General Procedure Hydrogenolysis. The compound (**9**/**10**/**11**/**12**/**13**/**14**/**15**/**16**/**21**/**22**/**23**/**24**) was dissolved in dry methanol and 20% $Pd(OH)_2$ on carbon (0.025 g per one benzyl group) and purged with hydrogen gas. The reaction mixture was stirred at RT for 2−3 days. The mixture was filtered through celite, and the filtrate was evaporated under reduced pressure. The residue was purified through a bond elute C-18 column eluted with water. The sulfated compound was passed through sodium (Na^+) resin. The product fraction was lyophilized to afford sulfated compounds as a white powder.

*Ethoxy-2-azidoethoxyl-O-(benzyl(2-O-benzoyl-3-O-benzyl-4-hydroxyl))-α-L-idopyranosideuronate (**5**).* The preparation of the target compound **5** (**82%**) was carried out from compound **L-1** according to the general lev deprotection procedure, and it was obtained as a syrup. ^{1}H NMR (400 MHz, chloroform-*d*): δ 8.00 (dd, *J* = 8.3, 1.4 Hz, 2H), 7.62−7.57 (m, 1H), 7.48−7.43 (m, 2H), 7.40−7.28 (m, 10H), 5.32 (d, *J* = 12.3 Hz, 1H), 5.27−5.26 (m, 1H), 5.24 (d, *J* = 12.3 Hz, 1H), 5.17 (s, 1H), 5.02 (d, *J* = 1.7 Hz, 1H), 4.84 (d, *J* = 11.6 Hz, 1H), 4.65 (d, *J* = 11.6 Hz, 1H), 4.16−4.12 (m, 1H), 3.98−3.93 (m, 1H), 3.89 (td, *J* = 3.0, 1.3 Hz, 1H), 3.76−3.67 (m, 3H), 3.63−3.53 (m, 2H), 3.19 (t, *J* = 5.0 Hz, 2H), and 2.80 (d, *J* = 11.6 Hz, 1H). ^{13}C NMR (101 MHz, chloroform-*d*): δ 169.54, 165.11, 137.70, 135.49, 133.84, 129.89, 129.14, 128.77, 128.73, 128.55, 128.52, 128.44, 128.02, 127.88, 99.00, 74.75, 72.16, 70.33, 70.25, 68.48, 68.29, 67.96, 67.47, 67.17, and 50.83. HRMS *m*/*z*: calcd for $C_{31}H_{33}N_3O_9Na$, 614.2114; found, 614.2114.

*Ethoxy-2-azidoethoxyl-O-(3-O-benzyl)-α-L-idopyranoside Uronic Acid (**9**).* The preparation of the target compound **9** (**90%**) was carried out from compound **5** according to the general deprotection of ester procedure, and it was obtained as a sticky solid. ^{1}H NMR (400 MHz, Methanol-d_4): δ 7.41−7.25 (m, 5H), 4.75−4.71 (m, 2H), 4.65−4.60 (m, 1H), 4.08 (s, 1H), 3.93−3.87 (m, 1H), 3.81−3.80 (m, 1H), 3.71−3.66 (m, 5H), 3.64−3.56 (m, 1H), and 3.23 (t, *J* = 4.9 Hz, 2H). ^{13}C NMR (101 MHz, Methanol-d_4): δ 173.88, 139.69, 129.32, 128.86, 128.67, 102.77, 78.04, 72.92, 71.28, 71.21, 69.92, 69.67, 69.24, 68.10, and 51.75. HRMS *m*/*z*: calcd for $C_{17}H_{23}N_3O_8Na$, 420.1383; found, 420.1381.

*Ethoxy-2-azidoethoxyl-O-(benzyl (2-O-benzoyl-3-O-benzyl-4-O-sulfonato))-α-L-idopyranosideuronate (**17**).* The preparation of the target compound **17** (**92%**) was carried out from compound **5** according to the general sulfation procedure, and it was obtained as a solid. ^{1}H NMR (400 MHz, Methanol-d_4): δ 8.17 (dd, *J* = 8.4, 1.3 Hz, 2H), 7.61−7.57 (m, 1H), 7.47 (ddd, *J* = 8.6, 4.4, 2.8 Hz, 4H), 7.40−7.32 (m, 5H), 7.30−7.22 (m, 3H), 5.37 (d, *J* = 12.0 Hz, 1H), 5.15−5.10 (m, 2H), 5.09 (d, *J* = 2.3 Hz, 1H), 5.07 (s, 1H), 4.81−4.76 (m, 2H), 4.65 (d, *J* = 60.6 Hz, 1H), 4.39 (ddd, *J* = 3.5, 2.7, 1.1 Hz, 1H), 3.88−3.83 (m, 1H), 3.70−3.62 (m, 3H), 3.59−3.46 (m, 2H), and 3.09 (t, *J* = 5.1 Hz, 2H). ^{13}C NMR (101 MHz, Methanol-d_4): δ 170.70, 167.13, 139.36, 136.96, 134.34, 131.33, 130.94, 129.77, 129.49, 129.46, 129.28, 128.99, 128.70, 99.71, 74.93, 73.48, 73.08, 71.27, 71.11, 69.43, 68.97, 68.51, 68.46, and 51.70. HRMS *m*/*z*: calcd for $C_{31}H_{33}N_3O_{12}S^-$, 670.1712; found, 670.1701.

*Ethoxy-2-azidoethoxyl-O-(-3-O-benzyl-4-O-sulfonato)-α-L-idopyranoside Uronic Acid (**21**).* The preparation of the target compound **21** (**85%**) was carried out from compound **17** according to the general deprotection of ester procedure, and it was obtained as a sticky solid. ^{1}H NMR (400 MHz, deuterium oxide): δ 7.52−7.41 (m, 5H), 4.92 (dd, *J* = 2.0, 0.9 Hz, 1H), 4.83 (d, *J* = 11.7 Hz, 1H), 4.70 (d, *J* = 11.6 Hz, 1H), 4.61 (d, *J* = 2.3 Hz, 1H), 4.20 (td, *J* = 3.3, 1.0 Hz, 1H), 3.93−3.87 (m, 1H), 3.76−3.68 (m, 6H), and 3.44−3.42 (m, 2H). ^{13}C NMR (101 MHz, deuterium oxide): δ 174.75, 137.21, 128.63, 128.62, 128.32, 100.31, 74.72, 73.42, 72.37, 69.48, 69.30, 67.75, 67.47, 67.38, and 50.13. HRMS *m*/*z*: calcd for $C_{17}H_{22}N_3O_{11}S^-$, 476.0981; found, 476.0989.

*Ethaoxy-2-aminoethoxyl-O-α-L-idopyranoside Uronic Acid (**I-10**).* The preparation of the target compound **I-10** (**86%**) was carried out from compound **9** according to the general hydrogenolysis procedure, and it was obtained as a white solid. ^{1}H NMR (400 MHz, deuterium oxide): δ 4.86 (d, *J* = 4.2 Hz, 1H), 4.62 (d, *J* = 3.6 Hz, 1H), 3.91−3.86 (m, 2H), 3.74 (dd, *J* = 6.9, 5.1 Hz, 2H), 3.71−3.68 (m, 4H), 3.51 (dd, *J* = 6.4, 4.2 Hz, 1H), and 3.14 (t, *J* = 5.1 Hz, 2H). ^{13}C NMR (101 MHz, deuterium oxide): δ 173.78, 101.00, 71.07, 70.15, 69.96, 69.85, 69.67, 67.92, 66.34, and 39.08. HRMS *m*/*z*: calcd for $C_{10}H_{19}O_8NNa$, 304.1008; found, 304.1001.

*Ethoxy-2-aminoethoxyl-O-(4-O-sulfonato)-α-L-idopyranoside Uronic Acid (**I-11**).* The preparation of the target compound **I-11** (**88%**) was carried out from compound **21** according to the general hydrogenolysis procedure, and it was obtained as a white solid. ^{1}H NMR (400 MHz, deuterium oxide): δ 4.78 (d, *J* = 3.5 Hz, 1H), 4.46 (d, *J* = 3.1 Hz, 1H), 4.41−4.39 (m, 1H), 4.11 (t, *J* = 5.0 Hz, 1H), 3.80−3.75 (m, 1H), 3.67 (dt, *J* = 11.8, 4.2 Hz, 1H), 3.62−3.59 (m, 4H), 3.47−3.45 (m, 1H), and 3.07−3.04 (m, 2H). ^{13}C NMR (101 MHz, deuterium oxide): δ 174.64, 100.66, 76.67, 69.84, 69.66, 69.00, 68.92, 67.79, 66.29, and 39.10. HRMS *m*/*z*: calcd for $C_{10}H_{18}NO_{11}S^-$, 360.0606; found, 360.0611.

*Ethoxy-2-azidoethoxyl-O-(2,4-O-disulfonato-3-O-benzyl)-α-L-idopyranosideuronic Acid (**13**).* The preparation of the target compound **13** (**75%**) was carried out from compound **9** according to the general sulfation procedure, and it was obtained as a solid. ^{1}H NMR (400 MHz, deuterium oxide): δ 7.49−7.36 (m, 5H), 5.10 (s, 1H), 4.76−4.71 (m, 3H), 4.64 (d, *J* = 1.7 Hz, 1H), 4.34 (dd, *J* = 2.3, 1.1 Hz, 1H), 4.33−4.32 (m, 1H), 3.89−3.83 (m, 1H), 3.76−3.70 (m, 3H), 3.68−3.62 (m, 2H), and 3.38−3.36 (m, 2H). ^{13}C NMR (101 MHz, deuterium oxide): δ 174.22, 136.95, 128.69, 128.63, 128.41, 98.50z, 72.98, 72.31, 71.92, 71.17, 69.49, 69.42, 67.57, 66.33, and 50.18. HRMS *m*/*z*: calcd for $C_{17}H_{21}N_3O_{14}S_2^{2-}$, 277.5238; found, 277.5333.

*Ethoxy-2-aminoethoxyl-O-(2,4-O-disulfonato)-α-L-idopyranoside Uronic Acid (**I-12**).* The preparation of the target compound **I-12** (**91%**) was carried out from compound **13** according to the general hydrogenolysis procedure, and it was obtained as a white solid. ^{1}H NMR (400 MHz, deuterium oxide): δ 5.14 (s, 1H), 4.59 (d, *J* = 2.0 Hz, 1H), 4.57 (d, *J* = 2.8 Hz, 1H), 4.48 (dt, *J* = 2.8, 1.4 Hz, 1H), 4.21 (dt, *J* = 2.5, 1.2 Hz, 1H), 3.84 (ddd, *J* = 13.9, 8.6, 4.4 Hz, 2H), 3.73 (q, *J* = 4.7, 4.2 Hz, 4H), and 3.20−3.18 (m, 2H). ^{13}C NMR (101 MHz, deuterium oxide): δ 174.88, 98.67, 74.60, 73.28, 69.86, 67.51, 66.46, 66.37, 66.26, and 39.18. HRMS *m*/*z*: calcd for $C_{10}H_{27}NO_{14}S_2^{2-}$, 219.5051; found, 219.5050.

*Ethoxy-2-azidoethoxyl-O-(benzyl(2-O-benzoyl-3-O-benzyl)-α-L-idopyranosyluronate-α(1 → 4) benzyl(2-O-benzoyl-3-O-benzyl))-α-L-idopyranosideuronate (**6**).* The preparation of the target compound **6** (**87%**) was carried out from compound **L-2** according to the general lev deprotection procedure, and it was obtained as a syrup. ^{1}H NMR (400 MHz, chloroform-*d*): δ 8.03 (ddd, *J* = 11.1, 8.3, 1.4 Hz, 4H), 7.71−7.66 (m, 1H), 7.55−7.48 (m, 5H), 7.42−7.33 (m, 12H), 7.32−7.26 (m, 6H), 7.24−7.71 (m, 2H), 5.40 (d, *J* = 12.2 Hz, 1H), 5.33 (t, *J* = 2.8 Hz, 1H), 5.29−5.25 (m, 4H), 5.23 (d, *J* = 12.3 Hz, 1H), 5.06 (d, *J* = 3.1 Hz, 1H), 4.96 (d, *J* = 1.7 Hz, 1H), 4.89 (dd, *J* = 11.8, 6.9 Hz, 2H), 4.78 (d, *J* = 11.3 Hz, 1H), 4.62 (dd, *J* = 24.6, 11.3 Hz, 2H), 4.32 (t, *J* = 3.5 Hz, 1H), 4.09−4.03 (m, 2H), 3.94−3.88 (m, 2H), 3.82−3.73 (m, 3H), 3.69−3.59 (m, 2H), 3.23 (td, *J* = 5.0, 4.3, 1.3 Hz, 2H), and 2.71 (d, *J* = 10.3 Hz, 1H). ^{13}C NMR (101 MHz, chloroform-*d*): δ 169.24, 168.86, 165.72, 164.80, 137.82, 137.23, 135.27, 135.22, 133.84, 133.37, 130.17, 129.96, 129.12, 129.08, 128.80, 128.73, 128.67, 128.64, 128.62, 128.55, 128.52, 128.42, 128.35, 128.33, 128.20, 127.91, 127.77, 101.77, 98.97, 75.64, 74.39, 72.87, 72.20, 70.29, 70.25, 68.65, 68.59, 68.50, 68.43, 67.38, 67.05, and 50.80. HRMS *m*/*z*: calcd for $C_{58}H_{57}N_3O_{16}Na$, 1074.3637; found, 1074.3633.

*Ethoxy-2-azidoethoxyl-O-((3-O-benzyl)-L-idopyranosyl Uronic Acid-α(1 → 4)(3-O-benzyl))-α-L-idopyranoside Uronic Acid (**10**).* The preparation of the target compound **10** (**73%**) was carried out from compound **6** according to the general deprotection of esters procedure, and it was obtained as a solid. ^{1}H NMR (400 MHz, Methanol-d_4): δ 7.47−7.24 (m, 10H), 5.05 (d, *J* = 1.9 Hz, 1H), 4.94−4.93 (m, 1H), 4.86 (d, *J* = 2.2 Hz, 1H), 4.83 (d, *J* = 1.7 Hz, 1H), 4.66−4.58 (m, 4H), 4.29−4.28 (m, 1H), 4. (p, *J* = 1.8 Hz, 2H), 3.94−3.88 (m, 1H), 3.77 (t, *J* = 3.4 Hz, 1H), 3.73 (dt, *J* = 2.7, 1.3 Hz, 1H), 3.71−3.56 (m, 7H), and 3.25 (t, *J* = 4.9 Hz, 2H). ^{13}C NMR (101

https://dx.doi.org/10.1021/acs.jmedchem.0c01800
J. Med. Chem. 2021, 64, 3367−3380

MHz, Methanol-d_4): δ 173.17, 173.01, 139.35, 138.89, 129.53, 129.51, 129.39, 129.02, 128.75, 104.09, 102.87, 76.69, 76.58, 76.10, 73.26, 73.17, 71.28, 71.24, 69.62, 69.37, 69.15, 68.59, 68.57, 67.19, and 51.80. HRMS m/z: calcd for $C_{30}H_{37}N_3O_{14}Na$, 686.2173; found, 686.2189.

*Ethoxy-2-azidoethoxyl-O-(benzyl(2-O-benzoyl-3-O-benzyl-4-O-sulfonato)-L-idopyranosyluronate-α(1 → 4)benzyl(2-O-benzoyl-3-O-benzyl))-α-L-idopyranosideuronate (**18**).* The preparation of the target compound **18** (87%) was carried out from compound **6** according to the general sulfation procedure, and it was obtained as a sticky solid. ^{1}H NMR (400 MHz, Methanol-d_4): δ 8.14 (dd, J = 8.4, 1.3 Hz, 2H), 7.88 (dd, J = 8.4, 1.2 Hz, 2H), 7.62−7.57 (m, 1H), 7.49−7.45 (m, 2H), 7.42−7.33 (m, 5H), 7.27−7.15 (m, 18H), 5.24 (d, J = 12.1 Hz, 1H), 5.19 (d, J = 1.8 Hz, 2H), 5.17 (d, J = 2.9 Hz, 1H), 5.11−5.06 (m, 3H), 5.00 (d, J = 3.3 Hz, 1H), 4.95 (d, J = 12.2 Hz, 1H), 4.90 (d, J = 2.8 Hz, 1H), 4.74 (d, J = 11.0 Hz, 1H), 4.66 (t, d, J = 3.3 Hz, 1H), 4.64 (d, J = 11.1 Hz, 1H), 4.58 (s, 2H), 4.56−4.47 (m, 2H), 4.38 (dt, J = 3.9, 2.0 Hz, 1H), 4.19 (t, J = 3.6 Hz, 1H), 3.99 (t, J = 3.6 Hz, 1H), 3.89 (ddd, J = 10.4, 5.5, 3.2 Hz, 1H), 3.70−3.64 (m, 1H), 3.63−3.60 (m, 2H), 3.57−3.46 (m, 2H), and 3.11 (t, J = 5.0 Hz, 2H). ^{13}C NMR (101 MHz, Methanol-d_4): δ 170.85, 169.99, 166.98, 166.97, 139.02, 138.92, 136.80, 136.69, 134.37, 134.35, 131.41, 130.99, 130.95, 130.27, 129.76, 129.68, 129.60, 129.51, 129.46, 129.43, 129.30, 129.25, 129.12, 129.08, 128.81, 128.72, 102.17, 99.96, 77.50, 76.81, 75.13, 74.07, 73.67, 73.58, 71.19, 71.12, 70.35, 69.88, 69.57, 69.54, 69.02, 68.38, and 51.70. HRMS m/z: calcd for $C_{58}H_{56}N_3O_{19}S^-$, 1130.3234; found, 1130.3226.

*Ethoxy-2-azidoethoxyl-O-((3-O-benzyl-4-O-sulfonato)-L-idopyranosyl Uronic Acid-α(1 → 4)(3-O-benzyl))-α-L-idopyranoside Uronic Acid (**22**).* The preparation of the target compound **22** (58%) was carried out from compound **18** according to the general deprotection of esters procedure, and it was obtained as a solid. ^{1}H NMR (400 MHz, Methanol-d_4): δ 7.46−7.22 (m, 10H), 5.07 (s, 1H), 4.90 (s, 1H), 4.76 (d, J = 12.2 Hz, 2H), 4.63 (t, J = 13.9 Hz, 4H), 4.44 (s, 1H), 4.17 (s, 1H), 3.90−3.87 (m, 1H), 3.77 (s, 1H), 3.711−3.55 (m, 7H), and 3.17 (t, J = 4.2 Hz, 2H). ^{13}C NMR (101 MHz, Methanol-d_4): δ 176.72, 170.27, 139.66, 138.82, 129.66, 129.45, 129.27, 128.96, 128.86, 128.54, 103.28, 102.98, 77.31, 76.36, 75.05, 73.28, 72.89, 72.85, 71.32, 71.23, 69.60, 69.14, 68.74, 68.07, 67.32, and 51.72. HRMS m/z: calcd for $C_{30}H_{36}N_3O_{17}S^-$, 742.1771; found, 742.1767.

*Ethoxy-2-aminoethoxyl-O-(α-L-idopyranosyl Uronic Acid-α(1 → 4))-α-L-idopyranosyl Uronic Acid (**I-20**).* The preparation of the target compound **I-20** (87%) was carried out from compound **10** according to the general hydrogenolysis procedure, and it was obtained as a white solid. ^{1}H NMR (400 MHz, deuterium oxide): δ 4.95 (d, J = 3.0 Hz, 1H), 4.89 (d, J = 3.4 Hz, 1H), 4.57 (d, J = 3.2 Hz, 1H), 4.55 (d, J = 2.7 Hz, 1H), 4.10−4.09 (m, 1H), 3.96−3.90 (m, 3H), 3.83−3.75 (m, 6H), 3.63−3.60 (m, 2H), and 3.23−3.20 (m, 2H). ^{13}C NMR (101 MHz, deuterium oxide): δ 176.14, 175.60, 102.36, 101.09, 78.52, 70.55, 70.40, 70.04, 69.86, 69.80, 69.29, 69.13, 68.82, 67.50, 66.29, and 39.08. HRMS m/z: calcd for $C_{16}H_{27}NO_{14}Na$, 480.1329 found, 480.1327.

*Ethoxy-2-aminoethoxyl-O-((4-O-sulfonato)-α-L-idopyranosyl Uronic Acid-α(1 → 4))-α-L-idopyranoside Uronic Acid (**I-21**).* The preparation of the target compound **I-21** (89%) was carried out from compound **22** according to the general hydrogenolysis procedure, and it was obtained as a white solid. ^{1}H NMR (400 MHz, deuterium oxide): δ 4.87 (dd, J = 4.4, 2.7 Hz, 2H), 4.66 (d, J = 2.4 Hz, 1H), 4.52 (t, J = 3.1 Hz, 1H), 4.47 (d, J = 2.7 Hz, 1H), 4.20 (t, J = 3.8 Hz, 1H), 4.01 (dd, J = 4.2, 2.8 Hz, 1H), 3.87−3.81 (m, 2H), 3.74−3.66 (m, 6H), 3.59 (ddd, J = 4.2, 2.3, 1.0 Hz, 1H), 3.53 (dd, J = 5.3, 3.0 Hz, 1H), and 3.14−3.12 (m, 1H). ^{13}C NMR (101 MHz, D_2O): δ 175.54, 174.70, 102.20, 101.13, 78.41, 76.12, 69.80, 69.12, 68.88, 68.30, 68.06, 67.92, 67.49, 66.30, and 39.09. HRMS m/z: calcd for $C_{16}H_{26}NO_{17}S^-$, 536.0927; found, 536.0899.

*Ethoxy-2-azidoethoxy-O-((2,4-O-disulfonato-3-O-benzyl)-α-L-idopyranosyl Uronic Acid-α(1 → 4)(2-O-sulfonato-3-O-benzyl))-α-L-idopyranoside Uronic Acid (**14**).* The preparation of the target compound **14** (72%) was carried out from compound **10** according to the general sulfation procedure, and it was obtained as a solid. ^{1}H NMR (400 MHz, deuterium oxide): δ 7.41−7.27 (m, 10H), 5.06 (s, 1H), 5.03 (s, 1H), 4.73 (d, J = 13.0 Hz, 2H), 4.68 (d, J = 7.5 Hz, 1H), 4.61 (dd, J = 12.0, 7.2 Hz, 2H), 4.42 (d, J = 1.9 Hz, 1H), 4.26−4.25 (m, 1H), 4.23−4.18 (m, 3H), 3.83 (d, J = 2.6 Hz, 1H), 3.76 (ddd, J = 7.4, 5.3, 3.1 Hz, 1H), 3.66−3.51 (m, 6H), and 3.27−3.25 (m, 2H). ^{13}C NMR (101 MHz, deuterium oxide): δ 175.18, 174.24, 137.15, 137.05, 128.68, 128.64, 128.56, 128.55, 128.30, 128.07, 100.61, 98.74, 75.90, 73.96, 72.88, 71.73, 71.56, 71.33, 71.27, 71.13, 69.41, 67.50, 67.25, 66.94, and 50.15. HRMS m/z: calcd for $C_{30}H_{34}N_3O_{23}S_3^{3-}$, 300.0254; found, 300.0245.

*Ethoxy-2-aminoethoxyl-O-((2,4-O-disulfonato)-α-L-idopyranosyl Uronic Acid-α(1 → 4)(2-sulfonato))-α-L-idopyroside Uronic Acid (**I-23**).* The preparation of the target compound **I-23** (85%) was carried out from compound **14** according to the general hydrogenolysis procedure, and it was obtained as a white solid. ^{1}H NMR (600 MHz, deuterium oxide): δ 5.05 (s, 2H), 4.76 (s, 1H), 4.54 (s, 1H), 4.47 (s, 1H), 4.40 (s, 1H), 4.13 (s, 1H), 4.09 (s, 1H), 3.96 (d, J = 8.8 Hz, 2H), 3.78−3.70 (m, 3H), 3.65−3.62 (m, 3H), and 3.09 (t, J = 5.1 Hz, 2H). ^{13}C NMR (151 MHz, D_2O): δ 174.96, 174.07, 100.74, 98.94, 77.93, 74.24, 74.03, 71.88, 69.80, 68.04, 67.61, 67.39, 66.21, 65.53, and 39.07. HRMS m/z: calcd for $C_{16}H_{24}NO_{23}S_3^{3-}$, 231.3306; found, 231.3313.

*Ethoxy-2-azidoethoxyl-O-(benzyl (2-O-benzoyl-3-O-benzyl)-α-L-idopyranosyl Uronate-α(1 → 4) Benzyl (2-O-benzoyl-3-O-benzyl)-L-idopyranosyl Uronate-α(1 → 4) Benzyl (2-O-benzoyl-3-O-benzyl))-α-L-idopyranoside Uronate (**7**).* The preparation of the target compound **7** (83%) was carried out from compound **L-3** according to the general lev deprotection procedure, and it was obtained as a syrup. ^{1}H NMR (400 MHz, chloroform-d): δ 7.97−7.88 (m, 6H), 7.59−7.55 (m, 1H), 7.44−7.37 (m, 6H), 7.35−7.27 (m, 9H), 7.26−7.16 (m, 14H), 7.16−7.06 (m, 9H), 5.31 (d, J = 3.1 Hz, 1H), 5.21 (t, J = 2.6 Hz, 2H), 5.17 (d, J = 2.3 Hz, 1H), 5.12 (d, J = 12.3 Hz, 1H), 5.07−4.97 (m, 6H), 4.95 (d, J = 2.9 Hz, 1H), 4.81 (d, J = 6.1 Hz, 1H), 4.79−4.76 (m, 3H), 4.71 (dd, J = 11.2, 5.5 Hz, 2H), 4.55 (dd, J = 15.3, 11.5 Hz, 2H), 4.44 (d, J = 10.8 Hz, 1H), 4.28 (t, J = 3.3 Hz, 1H), 4.17 (t, J = 3.2 Hz, 1H), 3.97−3.88 (m, 3H), 3.77−3.63 (m, 5H), 3.59−3.46 (m, 2H), 3.12 (t, J = 4.9 Hz, 2H), and 2.53 (d, J = 10.4 Hz, 1H). ^{13}C NMR (101 MHz, chloroform-d): δ 169.19, 168.78, 168.55, 16.70, 165.30, 164.61, 138.13, 137.37, 137.29, 135.35, 135.22, 134.99, 133.76, 133.41, 133.36, 130.33, 130.13, 129.91, 129.17, 129.11, 129.06, 128.74, 128.67, 128.65, 128.63, 128.56, 128.44, 128.42, 128.39, 128.34, 128.29, 128.28, 128.19, 128.15, 127.92, 127.80, 127.66, 101.77, 101.71, 98.97, 75.60, 75.22, 73.99, 72.88, 72.69, 72.00, 70.26, 70.24, 69.03, 68.74, 68.63, 68.53, 68.46, 68.43, 68.29, 68.13, 67.23, 67.08, 67.03, 67.00, and 50.79. HRMS m/z: calcd for $C_{85}H_{81}N_3O_{23}Na$, 1534.5159; found, 1534.5152.

*Ethoxy-2-azidoethoxyl-O-((3-O-benzyl)-α-L-idopyranosyl Uronic Acid-α(1 → 4)(3-O-benzyl)-α-L-idopyranosyl Uronic Acid-α(1 → 4)(3-O-benzyl))-α-L-idopyranoside Uronic Acid (**11**).* The preparation of the target compound **11** (75%) was carried out from compound **7** according to the general deprotection of esters procedure, and it was obtained as a sticky solid. ^{1}H NMR (400 MHz, Methanol-d_4): δ 7.40−7.27 (m, 15H), 5.00 (d, J = 4.0 Hz, 2H), 4.96 (d, J = 2.2 Hz, 1H), 4.86 (d, J = 2.4 Hz, 1H), 4.73 (d, J = 1.8 Hz, 1H), 4.69−4.63 (m, 2H), 4.59 (d, J = 7.5 Hz, 4H), 4.29 (t, J = 3.1 Hz, 1H), 4.23 (d, J = 3.7 Hz, 1H), 4.01 (d, J = 2.9 Hz, 1H), 3.94−3.89 (m, 1H), 3.80 (t, J = 3.8 Hz, 1H), 3.73−3.57 (m, 9H), 3.49 (s, 1H), and 3.25 (t, J = 5.0 Hz, 2H). ^{13}C NMR (101 MHz, Methanol-d_4): δ 173.11, 172.79, 172.36, 139.41, 138.69, 138.46, 129.84, 129.64, 129.60, 129.55, 129.39, 129.20, 129.13, 129.00, 128.75, 104.44, 104.18, 102.87, 76.83, 76.58, 76.22, 75.78, 74.89, 73.52, 73.33, 73.29, 71.27, 71.24, 69.58, 69.39, 68.94, 68.65, 68.63, 68.47, 67.63, 67.15, and 51.80. HRMS m/z: calcd for $C_{43}H_{51}N_3O_{20}Na$, 952.2964; found, 952.2944.

*Ethoxy-2-azidoethoxyl-O-(benzyl(2-O-benzoyl-3-O-benzyl-4-O-sulfonato)-α-L-idopyranosyl Uronate-α(1 → 4) Benzyl(2-O-benzoyl-3-O-benzyl)-L-idopyranosyl Uronate-α(1 → 4) Benzyl(2-O-benzoyl-3-O-benzyl))-α-L-idopyroside Uronate (**19**).* The preparation of the target compound **19** (87%) was carried out from compound **7** according to the general sulfation procedure, and it was obtained as a solid. ^{1}H NMR (400 MHz, Methanol-d_4): δ 8.06 (dd, J = 8.3, 1.1 Hz, 2H), 7.92−7.86 (m, 4H), 7.56−7.52 (m, 1H), 7.42−

https://dx.doi.org/10.1021/acs.jmedchem.0c01800
J. Med. Chem. 2021, 64, 3367−3380

7.34 (m, 6H), 7.28−7.05 (m, 33H), 5.25 (d, J = 3.8 Hz, 1H), 5.11−5.05 (m, 6H), 5.05−4.96 (m, 3H), 4.92−4.87 (m, 3H), 4.81 (d, J = 2.7 Hz, 1H), 4.72−4.59 (m, 5H), 4.52−4.45 (m, 2H), 4.39 (d, J = 11.0 Hz, 1H), 4.31 (t, J = 3.2 Hz, 1H), 4.19−4.18 (m, 1H), 4.13 (t, J = 2.8 Hz, 1H), 3.86 (ddt, J = 12.2, 7.5, 4.4 Hz, 3H), 3.67−3.58 (m, 3H), 3.55−3.43 (m, 2H), and 3.07 (t, J = 5.0 Hz, 2H). ^{13}C NMR (101 MHz, Methanol-d_4): δ 170.72, 170.14, 169.82, 166.93, 166.87, 166.68, 139.30, 139.01, 138.73, 136.95, 136.63, 136.59, 134.52, 134.46, 134.31, 131.40, 131.18, 131.03, 130.96, 130.49, 130.39, 129.73, 129.58, 129.56, 129.55, 129.50, 129.44, 129.42, 129.35, 129.33, 129.30, 129.27, 129.07, 129.02, 128.85, 128.77, 128.72, 102.59, 101.75, 100.00, 77.77, 77.14, 77.06, 76.28, 75.12, 74.19, 73.83, 73.66, 73.61, 71.22, 71.13, 70.64, 70.48, 69.91, 69.59, 69.56, 69.48, 69.07, 68.27, 68.22, 68.12, and 51.73. HRMS m/z: calcd for $C_{85}H_{80}N_3O_{26}S^-$, 1590.4756; found, 1590.4751.

*Ethoxy-2-azidoethoxyl-O-((3-O-benzyl-4-O-sulfonato)-α-L-idopyranosyl Uronic Acid-α(1 → 4)(3-O-benzyl)-L-idopyranosyl Uronic Acid-α(1 → 4)(3-O-benzyl))-α-L-idopyranoside Uronic Acid (**23**).* The preparation of the target compound **23** (**56%**) was carried out from compound **19** according to the general deprotection of ester procedure, and it was obtained as a sticky solid. ^{1}H NMR (400 MHz, Methanol-d_4): δ 7.44−7.24 (m, 15H), 5.15 (d, J = 3.6 Hz, 2H), 4.86 (d, J = 2.9 Hz, 1H), 4.72−4.52 (m, 11H), 4.25 (t, J = 2.5 Hz, 1H), 3.93−3.90 (m, 1H), 3.82 (d, J = 3.5 Hz, 1H), 3.73 (t, J = 3.1 Hz, 1H), 3.69−3.56 (m, 8H), 3.18 (ddd, J = 5.6, 4.2, and 1.0 Hz, 2H). ^{13}C NMR (101 MHz, MeOD): δ 176.72, 176.14, 175.28, 139.79, 139.22, 138.76, 129.82, 129.60, 129.45, 129.30, 129.24, 128.91, 128.70, 128.49, 103.80, 103.07, 102.74, 76.96, 75.80, 75.51, 74.75, 74.32, 73.68, 72.96, 72.90, 72.72, 71.30, 71.28, 69.92, 69.33, 69.02, 68.82, 68.41, 68.20, 67.87, and 51.74. HRMS m/z: calcd for $C_{43}H_{50}N_3O_{23}S^-$, 1008.2561; found, 1008.2558.

*Ethoxy-2-aminoethoxyl-O-(α-L-idopyranosyl Uronic Acid-α(1 → 4)-α-L-idopyranosyl Uronic Acid-α(1 → 4))-α-L-idopyranoside Uronic Acid (**I-30**).* The preparation of the target compound **I-30** (**85%**) was carried out from compound **11** according to the general hydrogenolysis procedure, and it was obtained as a white solid. ^{1}H NMR (400 MHz, deuterium oxide): δ 4.95 (d, J = 2.4 Hz, 2H), 4.90 (d, J = 3.1 Hz, 1H), 4.67 (d, J = 2.1 Hz, 1H), 4.57 (d, J = 2.8 Hz, 1H), 4.55 (d, J = 2.4 Hz, 1H), 4.11 (dt, J = 11.6, 3.1 Hz, 2H), 3.94 (ddd, J = 15.7, 8.6, 4.2 Hz, 4H), 3.82 (q, J = 4.3 Hz, 2H), 3.78−3.74 (m, 4H), 3.63 (dd, J = 8.0, 4.8 Hz, 3H), and 3.21 (t, J = 5.1 Hz, 2H). ^{13}C NMR (101 MHz, D_2O): δ 176.11, 175.61, 175.55, 102.50, 102.41, 101.09, 77.97, 77.87, 70.23, 70.18, 70.15, 69.82, 69.50, 68.88, 68.52, 68.35, 68.13, 67.47, 66.27, and 39.08. HRMS m/z: calcd for $C_{22}H_{35}NO_{20}Na$, 656.1650; found, 656.1659.

*Ethoxy-2-aminoethoxyl-O-((4-O-sulfonato)-α-L-idopyranosyl Uronic Acid-α(1 → 4)-L-idopyranosyl Uronic Acid-α(1 → 4))-α-L-idopyranoside Uronic Acid (**I-31**).* The preparation of the target compound **I-31** (**86%**) was carried out from compound **23** according to the general hydrogenolysis procedure, and it was obtained as a white solid. ^{1}H NMR (400 MHz, deuterium oxide): δ 4.87 (dd, J = 5.6, 2.3 Hz, 3H), 4.67 (d, J = 2.4 Hz, 1H), 4.59 (d, J = 2.3 Hz, 1H), 4.51 (t, J = 3.0 Hz, 1H), 4.47 (d, J = 2.4 Hz, 1H), 4.19 (td, J = 3.8, 1.0 Hz, 1H), 4.02 (dt, J = 10.4, 3.2 Hz, 2H), 3.82 (q, J = 5.0 Hz, 2H), 3.74−3.65 (m, 5H), 3.58 (ddd, J = 3.9, 2.2, 1.0 Hz, 1H), 3.55−3.51 (m, 2H), and 3.15−3.09 (m, 1H). ^{13}C NMR (101 MHz, D_2O): δ 175.51, 175.38, 174.38, 102.56, 102.29, 101.10, 78.00, 77.89, 75.84, 69.81, 69.53, 68.88, 68.53, 68.45, 68.18, 68.04, 67.82, 67.65, 67.48, 66.28, and 39.08. HRMS m/z: calcd for $C_{22}H_{34}NO_{23}S^-$, 712.1248; found, 712.1229.

*Ethoxy-2-aminoethoxyl-O-((2,4-O-disulfonato-3-O-benzyl)-α-L-idopyranosyl Uronic Acid-α(1 → 4)(2-O-sulfonato-3-O-benzyl)-α-L-idopyranosyl Uronic Acid-α(1 → 4)(2-O-sulfonato-3-O-benzyl))-α-L-idopyranoside Uronic Acid (**15**).* The preparation of the target compound **15** (**70%**) was carried out from compound **11** according to the general sulfation procedure, and it was obtained as a solid. ^{1}H NMR (400 MHz, deuterium oxide): δ 7.42−7.26 (m, 15H), 5.10 (d, J = 9.3 Hz, 2H), 5.03 (s, 1H), 4.75 (d, J = 2.9 Hz, 1H), 4.73−4.61 (m, 3H), 4.68−4.59 (m, 5H), 4.42 (d, J = 1.9 Hz, 1H), 4.31 (s, 1H), 4.23 (d, J = 10.6 Hz, 8H), 3.87 (s, 2H), 3.77 (dt, J = 10.6, 3.6 Hz, 1H), 3.68−3.52 (m, 5H), and 3.30−3.28 (m, 2H). ^{13}C NMR (101 MHz, deuterium oxide): δ 175.24, 174.71, 174.11, 137.24, 137.21, 137.17, 128.73, 128.71, 128.69, 128.61, 128.57, 128.30, 128.09, 100.82, 100.34, 98.88, 76.11, 74.54, 74.09, 72.85, 72.69, 72.12, 71.91, 71.71, 71.28, 71.24, 70.90, 70.89, 69.46, 69.43, 67.54, 67.33, 67.07, and 50.19. HRMS m/z: calcd for $C_{43}H_{47}N_3O_{32}S_4^{4-}$, 311.2762; found, 311.2769.

*Ethoxy-2-aminoethoxyl-O-(2,4-O-disulfonato)-α-L-idopyranosyl uronic acid-α(1 → 4)(2-O-sulfonato)-α-L-idopyranosyl uronic acid-α(1 → 4)(2-O-sulfonato)-α-L-idopyranoside uronic acid (**I-34**).* The preparation of the target compound **I-34** (**83%**) was carried out from compound **15** according to the general hydrogenolysis procedure, and it was obtained as a white solid. ^{1}H NMR (600 MHz, deuterium oxide): δ 5.19 (s, 1H), 5.17−5.16 (m, 2H), 4.68 (t, J = 2.3 Hz, 2H), 4.57 (d, J = 2.1 Hz, 1H), 4.52 (td, J = 2.6, 1.2 Hz, 1H), 4.27 (dt, J = 2.4, 1.2 Hz, 1H), 4.25 (dd, J = 2.6, 1.3 Hz, 1H), 4.21 (t, J = 2.9 Hz, 1H), 4.17 (t, J = 2.4 Hz, 1H), 4.09−4.07 (m, 3H), 3.90−3.82 (m, 1H), 3.80−3.72 (m, 5H), and 3.22−3.21 (m, 2H). ^{13}C NMR (151 MHz, D_2O): δ 175.13, 174.92, 174.36, 100.79, 99.00, 77.75, 77.01, 74.33, 72.22, 71.67, 69.89, 68.14, 67.71, 67.47, 67.31, 67.14, 66.53, 66.29, 65.56, and 39.16. HRMS m/z: calcd for $C_{22}H_{31}NO_{32}S_4^{4-}$, 237.2433; found, 237.2439.

*Ethoxy-2-azidoethoxyl-O-(benzyl(2-O-benzoyl-3-O-benzyl))-α-L-idopyranosyl Uronate-α(1 → 4) Benzyl (2-O-benzoyl-3-O-benzyl)-α-L-idopyranosyl Uronate-α(1 → 4) Benzyl (2-O-benzoyl-3-O-benzyl)-α-L-idopyranosyl Uronate-α(1 → 4) Benzyl (2-O-benzoyl-3-O-benzyl)-α-L-idopyranoside Uronate (**8**).* The preparation of the target compound **8** (**85%**) was carried out from compound **L-4** according to the general lev deprotection procedure, and it was obtained as a syrup. ^{1}H NMR (400 MHz, chloroform-d): δ 7.95−7.91 (m, 4H), 7.86 (ddd, J = 13.4, 8.2, 1.0 Hz, 4H), 7.59−7.54 (m, 1H), 7.42−7.33 (m, 8H), 7.32−7.22 (m, 15H), 7.20−7.13 (m, 15H), 7.12−7.03 (m, 11H), 6.96 (dd, J = 6.6, 3.0 Hz, 2H), 5.22 (dd, J = 5.3, 2.9 Hz, 2H), 5.18−5.14 (m, 4H), 5.11−5.00 (m, 6H), 4.92 (d, J = 3.0 Hz, 1H), 4.81−4.71 (m, 6H), 4.67 (d, J = 3.5 Hz, 1H), 4.65−4.56 (m, 3H), 4.51 (dd, J = 17.0, 11.5 Hz, 2H), 4.41 (d, J = 11.1 Hz, 1H), 4.33 (d, J = 11.4 Hz, 1H), 4.21 (t, J = 3.2 Hz, 1H), 4.13 (t, J = 2.9 Hz, 1H), 4.06 (t, J = 2.9 Hz, 1H), 3.98 (t, J = 2.9 Hz, 1H), 3.96−3.91 (m, 1H), 3.89 (t, J = 3.7 Hz, 1H), 3.82−3.81 (m, 1H), 3.71−3.62 (m, 5H), 3.57−3.46 (m, 2H), 3.11−3.08 (m, 2H), and 2.49 (d, J = 10.3 Hz, 1H). ^{13}C NMR (101 MHz, $CDCl_3$): δ 169.19, 168.69, 168.58, 168.31, 165.66, 165.33, 165.12, 164.64, 138.07, 137.74, 137.41, 137.33, 135.33, 135.22, 135.07, 135.04, 133.79, 133.37, 133.33, 130.34, 130.22, 130.03, 129.91, 129.24, 129.18, 129.02, 128.99, 128.92, 128.66, 128.60, 128.57, 128.56, 128.49, 128.47, 128.39, 128.36, 128.32, 128.29, 128.23, 128.21, 128.10, 127.88, 127.79, 127.77, 127.61, 102.05, 101.53, 101.41, 98.91, 76.49, 75.93, 75.59, 74.79, 73.46, 72.77, 72.67, 71.71, 70.24, 69.73, 68.99, 68.70, 68.58, 68.56, 68.39, 68.35, 67.63, 67.18, 66.93, 66.91, and 50.78. HRMS m/z: calcd for $C_{112}H_{105}N_3O_{30}Na$, 1994.6681; found, 1994.6678.

*Ethoxy-2-azidoethoxyl-O-((3-O-benzyl)-α-L-idopyranosyl Uronic Acid-α(1 → 4)(3-O-benzyl)-α-L-idopyranosyl Uronic Acid-α(1 → 4)(3-O-benzyl)-α-L-idopyranosyl Uronic Acid-α(1 → 4)(3-O-benzyl))-α-L-idopyranoside Uronic Acid (**12**).* The preparation of the target compound **12** (**68%**) was carried out from compound **8** according to the general ester deprotection procedure, and it was obtained as a sticky solid. ^{1}H NMR (400 MHz, Methanol-d_4): δ 7.42−7.27 (m, 20H), 5.03 (s, 1H), 4.99 (s, 1H), 4.96 (d, J = 2.1 Hz, 1H), 4.94 (s, 1H), 4.79 (d, J = 1.7 Hz, 1H), 4.70−4.69 (m, 1H), 4.66−4.61 (m, 4H), 4.58−4.53 (m, 4H), 4.31 (t, J = 3.2 Hz, 1H), 4.24−4.21 (m, 2H), 4.01 (dt, J = 3.4, 1.7 Hz, 1H), 3.95−3.89 (m, 1H), 3.80 (t, J = 3.7 Hz, 1H), 3.74 (t, J = 3.4 Hz, 1H), 3.71−3.62 (m, 10H), 3.61−3.55 (m, 3H), 3.53 (dt, J = 2.7, 1.2 Hz, 1H), 3.40 (dt, J = 2.6, 1.2 Hz, 1H), and 3.25 (t, J = 5.0 Hz, 2H). ^{13}C NMR (101 MHz, MeOD): δ 173.43, 173.09, 172.66, 172.52, 139.62, 138.90, 138.78, 138.50, 130.13, 130.04, 129.89, 129.85, 129.81, 129.76, 129.60, 129.50, 129.40, 129.34, 129.22, 128.96, 104.74, 104.62, 104.44, 103.09, 77.02, 76.81, 76.41, 76.19, 76.03, 75.36, 74.83, 73.85, 73.73, 73.52, 71.49, 71.46, 69.82, 69.60, 69.14, 68.84, 68.71, 67.91, 67.37, 62.47, and 52.02. HRMS m/z: calcd for $C_{56}H_{65}N_3O_{26}Na$, 1195.3856; found, 1195.3861.

https://dx.doi.org/10.1021/acs.jmedchem.0c01800
J. Med. Chem. 2021, 64, 3367−3380

*Ethoxy-2-azidoethoxyl-O-(benzyl(2-O-benzoyl-3-O-benzyl-4-O-Sulfonato)-α-L-idopyranosyl Uronate-α(1 → 4) Benzyl (2-O-benzoyl-3-O-benzyl)-α-L-idopyranosyl Uronate-α(1 → 4) Benzyl (2-O-benzoyl-3-O-benzyl)-α-L-idopyranosyl Uronate-α(1 → 4)-benzyl (2-O-benzoyl-3-O-benzyl))-α-L-idopyranoside Uronate (**20**).* The preparation of the target compound **20** (**85%**) was carried out from compound **8** according to the general sulfation procedure, and it was obtained as a sticky solid. ^{1}H NMR (400 MHz, Methanol-d_4): δ 8.09 (d, *J* = 7.7 Hz, 2H), 7.96 (d, *J* = 7.8 Hz, 2H), 7.88 (dd, *J* = 10.3, 7.9 Hz, 4H), 7.57 (t, *J* = 7.4 Hz, 1H), 7.42 (dd, J = 17.4, 7.6 Hz, 6H), 7.29−7.13 (m, 37H), 7.09 (dd, *J* = 4.9, 2.5 Hz, 6H), 7.00−6.98 (m, 2H), 5.22 (t, *J* = 3.3 Hz, 2H), 5.09 (ddd, *J* = 15.2, 9.5, 3.5 Hz, 9H), 4.99−4.90 (m, 4H), 4.75−4.65 (m, 7H), 4.58 (t, *J* = 11.6 Hz, 2H), 4.49−4.38 (m, 4H), 4.33 (t, *J* = 3.3 Hz, 1H), 4.20 (t, J = 3.3 Hz, 1H), 4.11 (d, *J* = 3.2 Hz, 2H), 3.97 (t, *J* = 3.6 Hz, 1H), 3.89 (dt, *J* = 19.3, 4.3 Hz, 3H), 3.67−3.58 (m, 3H), 3.55−3.44 (m, 2H), and 3.08 (q, *J* = 4.8 Hz, 2H). ^{13}C NMR (101 MHz, MeOD): δ 170.79, 170.14, 169.87, 169.84, 166.88, 166.85, 166.67, 166.58, 139.26, 139.01, 138.94, 138.71, 136.92, 136.65, 136.60, 136.41, 134.65, 134.49, 134.48, 134.32, 131.41, 131.17, 131.16, 131.00, 130.92, 130.54, 130.37, 130.31, 129.85, 129.59, 129.57, 129.52, 129.50, 129.45, 129.42, 129.40, 129.38, 129.36, 129.32, 129.30, 129.26, 129.23, 129.14, 129.06, 128.99, 128.90, 128.81, 128.68, 102.74, 102.16, 101.63, 99.96, 77.95, 77.30, 77.20, 77.06, 76.60, 76.40, 74.76, 74.18, 73.89, 73.86, 73.53, 73.50, 71.20, 71.11, 70.96, 70.77, 70.23, 70.10, 69.95, 69.78, 69.49, 69.43, 68.80, 68.25, 68.23, 68.18, 67.96, and 51.70. HRMS *m*/*z*: calcd for $C_{112}H_{104}N_3O_{33}S^-$, 2050.6278; found, 2050.6282.

*Ethoxy-2-azidoethoxyl-O-((3-O-benzyl-4-O-sulfonato)-α-L-idopyranosyl Uronic Acid-α(1 → 4)(3-O-benzyl)-α-L-idopyranosyl Uronic Acid-α(1 → 4)(3-O-benzyl)-α-L-idopyranosyl Uronic Acid-α(1 → 4)(3-O-benzyl))-α-L-idopyranoside Uronic Acid (**24**).* The preparation of the target compound **24** (**56%**) was carried out from compound **20** according to the general ester deprotection procedure, and it was obtained as a solid. ^{1}H NMR (600 MHz, Methanol-d_4): δ 7.44−7.23 (m, 20H), 5.13 (d, *J* = 3.4 Hz, 2H), 5.10 (s, 1H), 4.88 (s, 2H), 4.84 (d, *J* = 5.2 Hz, 1H), 4.69−4.60 (m, 10H), 4.58−4.50 (m, 8H), 4.23 (t, *J* = 3.0 Hz, 1H), 3.90 (ddd, *J* = 10.5, 4.9, 3.2 Hz, 1H), 3.82 (d, *J* = 6.1 Hz, 1H), 3.73 (d, *J* = 6.2 Hz, 1H), 3.67−3.65 (m, 3H), 3.65−3.60 (m, 4H), 3.58 (dd, *J* = 6.1, 4.1 Hz, 1H), 3.57−3.56 (m, 1H), 3.51−3.50 (m, 1H), and 3.19−3.13 (m, 2H). ^{13}C NMR (151 MHz, MeOD): δ 176.76, 176.08, 175.94, 175.20, 139.79, 139.21, 138.79, 138.65, 129.92, 129.83, 129.65, 129.60, 129.49, 129.31, 129.26, 128.98, 128.93, 128.89, 128.71, 128.50, 103.95, 103.62, 103.02, 102.79, 76.86, 75.83, 75.41, 75.20, 74.57, 74.54, 74.13, 73.64, 72.98, 72.85, 72.81, 72.72, 71.35, 71.27, 69.81, 69.32, 69.22, 69.01, 68.71, 68.37, 68.29, 68.19, 67.86, and 51.71. HRMS *m*/*z*: calcd for $C_{56}H_{64}N_3O_{29}S^-$, 1274.3352; found, 1274.3342.

*Ethoxy-2-aminoethoxyl-O-(α-L-idopyranosyl uronic acid-α(1 → 4)-α-L-idopyranosyl uronic acid -α(1 → 4)-α-L-idopyranosyl uronic acid-α(1 → 4))-α-L-idopyranoside uronic acid (**I-40**).* The preparation of the target compound **I-40** (**82%**) was carried out from compound **12** according to the general hydrogenolysis procedure, and it was obtained as a white solid. ^{1}H NMR (600 MHz, deuterium oxide): δ 4.99−4.91 (m, 6H), 4.14 (d, *J* = 12.9 Hz, 3H), 4.03 (t, *J* = 3.8 Hz, 1H), 3.92 (dt, *J* = 9.8, 4.5 Hz, 3H), 3.84 (t, *J* = 5.2 Hz, 1H), 3.80−3.73 (m, 5H), 3.65−3.58 (m, 5H), and 3.20 (t, *J* = 5.0 Hz, 2H). ^{13}C NMR (151 MHz, D_2O): δ 173.00, 172.78, 172.72, 102.78, 102.74, 102.64, 101.12, 77.61, 77.58, 77.50, 70.02, 69.83, 69.62, 69.47, 69.25, 69.03, 68.96, 68.84, 68.56, 68.40, 68.05, 67.94, 67.70, and 39.01. HRMS *m*/*z*: calcd for $C_{28}H_{43}NO_{26}Na$, 832.1971; found, 832.1987.

*Ethoxy-2-aminoethoxyl-O-(4-O-sulfonato)-α-L-idopyranosyl Uronic Acid-α(1 → 4)-α-L-Idopyranosyl Uronic Acid-α(1 → 4)-α-L-idopyranosyl Uronic Acid-α(1 → 4)-α-L-idopyranoside Uronic Acid (**I-41**).* The preparation of the target compound **I-41** (**81%**) was carried out from compound **24** according to the general hydrogenolysis procedure, and it was obtained as a white solid. ^{1}H NMR (600 MHz, deuterium oxide): δ 4.90 (s, 1H), 4.87−4.54 (m, 3H), 4.65 (d, *J* = 8.2 Hz, 2H), 4.53−4.51 (m, 2H), 4.16 (t, *J* = 3.7 Hz, 1H), 4.03 (d, *J* = 14.3 Hz, 3H), 3.82 (p, *J* = 4.4 Hz, 4H), 3.72−3.63 (m, 5H), 3.58 (d, *J* = 4.1 Hz, 1H), 3.52 (dq, *J* = 5.2, 2.5 Hz, 3H), and 3.11 (t, *J* = 5.0 Hz, 2H). ^{13}C NMR (151 MHz, D_2O): δ 174.83, 174.64, 174.44, 173.09, 102.68, 102.42, 102.18, 101.00, 77.87, 77.76, 77.37, 75.18, 69.66, 69.34, 68.84, 68.64, 68.42, 68.31, 68.20, 68.07, 68.00, 67.82, 67.52, 67.43, 67.22, 66.18, and 38.94. HRMS *m*/*z*: calcd for $C_{28}H_{42}NO_{29}S^-$, 888.1569; found, 888.1556.

*Ethoxy-2-azidoethoxyl-O-((2-4-O-disulfonato-3-O-benzyl)-α-L-idopyranosyl Uronic Acid-α(1 → 4)(2-O-sulfonato-3-O-benzyl)-α-L-idopyranosyl Uronic Acid-α(1 → 4)(2-O-sulfonato-3-O-benzyl)-α-L-idopyranosyl Uronic Acid-α(1 → 4)(2-O-sulfonato-3-O-benzyl))-α-L-idopyranoside Uronic Acid (**16**).* The preparation of the target compound **16** (**70%**) was carried out from compound **12** according to the general sulfation procedure, and it was obtained as a solid. ^{1}H NMR (600 MHz, deuterium oxide): δ 753−738 (m, 20H), 5.24 (s, 2H), 5.17 (d, *J* = 33.8 Hz, 2H), 4.87−478 (m, 6H), 4.74 (d, *J* = 13.8 Hz, 5H), 4.67 (d, *J* = 12.3 Hz, 2H), 4.52 (s, 1H), 4.42 (s, 1H), 4.38−4.34 (m, 6H), 3.97 (d, *J* = 19.6 Hz, 3H), 3.89−3.87 (m, 1H), 3.78−3.67 (m, 5H), and 3.41−3.39 (m, 2H). ^{13}C NMR (151 MHz, D_2O): δ 175.20, 174.75, 174.57, 173.99, 137.19, 137.13, 128.72, 128.65, 128.57, 128.52, 128.24, 128.03, 100.75, 100.44, 100.00, 98.84, 76.14, 74.60, 74.07, 73.93, 72.82, 72.55, 72.39, 72.19, 71.84, 71.71, 71.65, 71.28, 71.17, 70.81, 70.72, 69.42, 69.38, 67.53, 67.49, 67.39, 67.31, 67.06, and 50.14. HRMS *m*/*z*: calcd for $C_{56}H_{60}N_3O_{41}S_5^{5-}$, 318.0267; found, 318.0266.

*Ethoxy-2-aminoethoxyl-O-((2-4-O-disulfonato)-α-L-idopyranosyl Uronic Acid-α(1 → 4)(2-O-sulfonato)-α-L-idopyranosyl Uronic Acid-α(1 → 4)(2-O-sulfonato)-α-L-idopyranosyl Uronic Acid-α(1 → 4)(2-O-sulfonato))-α-L-idopyranoside Uronic Acid (**I-45**).* The preparation of the target compound **I-45** (**81%**) was carried out from compound **12** according to the general hydrogenolysis procedure, and it was obtained as a white solid. ^{1}H NMR (600 MHz, deuterium oxide): δ 5.17−5.11 (m, 4H), 5.06 (t, *J* = 6.1 Hz, 3H), 4.78 (s, 1H), 4.57 (s, 1H), 4.35 (s, 1H), 4.13−4.03 (m, 10H), 3.81 (dt, *J* = 12.1, 4.0 Hz, 1H), 3.74 (dt, *J* = 12.1, 3.8 Hz, 1H), 3.67 (q, *J* = 7.3, 6.1 Hz, 4H), and 3.12 (t, *J* = 4.9 Hz, 2H). ^{13}C NMR (151 MHz, D_2O): δ 172.79, 172.36, 171.79, 102.17, 102.03, 101.97, 98.80, 78.81, 78.63, 78.53, 73.31, 73.15, 72.26, 69.63, 67.65, 67.03, 66.76, 66.61, 66.34, 65.57, and 39.09. HRMS *m*/*z*: calcd for $C_{28}H_{38}NO_{41}S_5^{5-}$, 240.7910; found, 240.7912.

Glycan Microarray. *Materials.* PBS 10× was purchased from Hylabs, ethanolamine from Fisher, and ovalbumin (Grade V), sodium phosphate monobasic monohydrate, sodium phosphate dibasic heptahydrate, Tween-20, and Tris/HCl were purchased from Sigma-Aldrich. Antibodies were purchased from Peprotech: Human SD1α CXCL12, human IL8 CXCL8 72 aa, human exodus-2 CCL21, human MCP-3 CCL7, human MCP-4 CCL13, human IP-10 CXCL10, human MEC CCL28, human RANTES CCL5, human MCP-1/MCAF CCL2, biotinylated antigen affinity-purified goat-anti-murine SDF-1α, biotinylated-rabbit-anti-human IL8 CXCL8, biotinylated-rabbit-anti-human Exodus-2 CCL21, biotinylated goat-anti-human MCP-3, biotinylated anti-H-MCP-4, biotinylated rabbit-anti-human IP-10, biotinylated anti-human MEC, and biotinylated-rabbit-anti-human MCAF/MCP-1. Biotinylated anti-Rantes was purchased from R&D. Cy3-sterptavidin (Cy3-SA) was purchased from Jackson ImmunoResearch.

Heparin-saccharide Microarray Fabrication. Arrays were fabricated with a NanoPrint LM-60 Microarray Printer (Arrayit) on epoxide-derivatized slides (PolyAn 2D) with 16 subarray blocks on each slide. Glycoconjugates were distributed into 384-well source plates using 4 replicate wells per sample and 7 μL per well. Each glycoconjugate was diluted into 50 and 100 μM in an optimized printing buffer (300 mM phosphate buffer, pH 8.4 Version VrHI.01). To monitor printing, Alexaflour-555-hydraside (Invitrogen, at 1 ng/μL in 178 mM phosphate buffer, pH 5.5) was used for each printing run. The arrays were printed with four 946MP3 pins (5 μm tip, 0.25 μL sample channel, ∼100 μm spot diameter; Arrayit). The humidity level in the arraying chamber was maintained at about 70% during printing. The printed slides were left on an arrayed deck overnight, allowing humidity to drop to ambient levels (40−45%). Next, the slides were packed, vacuum-sealed, and stored at RT until used.

https://dx.doi.org/10.1021/acs.jmedchem.0c01800
J. Med. Chem. 2021, 64, 3367−3380

Heparin-saccharide Microarray Binding Assay. Slides were developed and analyzed as previously described with some modifications.[58,59] Slides were rehydrated with dH_2O and incubated for 30 min in a staining dish with 50 °C prewarmed ethanolamine (0.05 M) in Tris−HCl (0.1 M, pH 9.0) to block the remaining reactive epoxy groups on the slide surface, then washed with 50 °C prewarmed dH_2O. Slides were centrifuged at 200*g* for 3 min, then fitted with the ProPlate Multi-Array 16-well slide module (Grace Bio-lab P37001) to divide into the subarrays (blocks). Slides were washed with PBST (0.1% Tween 20), aspirated, and blocked with 200 μL/subarray of blocking buffer (PBS pH 7.3 + 1% w/v ovalbumin) for 1 h at RT with gentle shaking. Next, the blocking solution was aspirated and 100 μL/block of primary detection proteins (for each detection, 3 serially decreasing concentrations were used, see Table S1) diluted in PBS pH 7.3 + 1% w/v ovalbumin were incubated with gentle shaking for 2 hours at RT. Slides were washed 4 times with PBST, then with PBS (without Tween-20) for 2 min. Bound antibodies were detected by incubating with biotinylated secondary detections (1 ng/μL, see Table S1) diluted in PBS, 200 μL/block at RT for 1 h. Slides were washed 4 times with PBST, then with PBS (without Tween-20) for 2 min and biotinylated antibodies were detected with Cy3-SA (1.2 μg/mL). Slides were washed 4 times with PBST, then with PBS for 10 min followed by removal from the ProPlate Multi-Array slide module and immediately dipping in a staining dish with dH_2O for 10 min with shaking. The slides were then centrifuged at 200*g* for 3 min. and the dry slides immediately scanned.

Array slide Processing. Processed slides were scanned and analyzed as described at 10 μm resolution with a Genepix 4000B microarray scanner (Molecular Devices) using 350 gain. Image analysis was carried out with Genepix Pro 4.0 analysis software (Molecular Devices). Spots were defined as circular features with a variable radius as determined by the Genepix scanning software. Local background subtraction was performed. RFU from each spot was calculated and ranking was used to compare the data between detections; each detection was tested at three dilutions. For each dilution, the binding RFUs of the glycans were listed, maximum RFU was determined and was set to be 100% binding so all others were calculated as a ratio to it (percent). Then, the rank for each glycan was averaged between the three dilutions and SEM was calculated.

Glycan Microarray Analysis of Binding Assay. Binding was tested at three serial dilutions, then detected with the relevant biotinylated secondary antibody (1 μg/mL) followed by Cy3-strepavidin (1.5 μg/mL), as in Table S1. Arrays were scanned and RFUs were calculated of chemokines binding to 100 μM glycans printed at four replicates. Rank binding of chemokines (each at three dilutions) to glycans printed at four replicates each was calculated. For each binding assay per printed block, the maximum RFU was determined and set as 100% binding. Then, binding to all other glycans in the same block was ranked in comparison to the maximal binding, and average rank binding (and SEM) for each glycan across the three examined concentrations of each chemokine was calculated. This analysis allowed to compare the glycan-binding profiles of the different chemokines and dissect their binding preferences.

Surface Plasmon Resonance Binding Kinetics. **I-45** was covalently immobilized on the sensor chip via coupling reaction. At first, the dextran matrix on CM5 chip was activated with NHS (0.02 M) and EDC coupling reagent (0.2 M) at a flow rate of 5 μL min^{-1} for 15 min before activating with 50 μL of **I-45** (0.5 mM) in HBS-EP buffer. In the negative control cell after EDC and NHS activation, 0.5 mM ethanol amine solution was flowed. The positive RU response on 1−45 confirmed immobilization of the HS ligand on CM5 chips. Then, different chemokines at a flow rate of 50 μL/min and 25 °C in HBS-EP buffer without chemokines were then flowed over the sensor surface for 3 min to enable association/dissociation. Kinetic analysis was performed using the BIAevaluation software for T100. Association and dissociation phase data were globally fitted to a simple 1:1 interaction model.

Cell Proliferation Assay. MCF-7 or MDA-MB-231 (approximately 10^4) was plated on 96-well plates in a RPMI-1640 medium in 1% FBS without growth supplements. Cells were incubated for 4 hr before the experiments. First, HS biomimetics (**I-45** and **I-41**, 10 or 50 μg/mL) and native heparin (10 or 50 μg/mL) were preincubated with CCL2 (50 ng/mL) and added to the cells. After 48 h of incubation, cells were washed and fixed with paraformaldehyde. Cells were stained with 4% sulforhodamine B in 1% acetic acid for 30 min and washed with 1% acetic acid solution. Cell proliferation was determined with 2-(4-iodophenyl)-3-(4-nitrophenyl)-5-(2,4-disulfophenyl)-2*H*-tetrazolium monosodium salt at 450 nm.

Cell-division Cycle Analysis. MCF-7 cells were treated with chemokines and HS mimetics as mentioned above after 72 h, cells were harvested and fixed overnight in 70% ethanol at −20 °C. The cells were then incubated with RNase (10 μg/mL) and propidium iodide (5 μg/mL) for 30 min at 37 °C. The stained cells were analyzed with a flow cytometer. The G0/G1, S, and G2/M phases of the DNA content were quantified by using ModFitLT version 3.0 software.

Wound Healing Assay. MCF-7 cells were cultured on 24-well plates in RPMI-1640 medium. After monolayer formation, a wound was created by scratching the monolayer with a 1000 μL pipette tip. Cells were starved with Heparin and its mimetics (**I-45**, **I-41**; 10 or 50 μg/mL) with CCL2 (50 ng). After 8 h, CCL2-treated monolayer showed complete wound healing. At that point, the percent of cell migration distance of heparin mimetics-treated cells were quantified.

Cell Invasion Assay. Cell invasion assay was performed in 24-well boyden chamber inserts with 8 μM pores. The upper chambers of transwell inserts were coated with mAtrigel. The bottom chamber contained 600 μL RPMI-1640 medium supplemented with 1% FBS and CCL2 (50 ng/mL) with heparin mimetics (**I-45**, **I-41**, and heparin). MCF-7 cells were added to the upper chamber. After 24 h incubation at 37 °C, non-invading cells were removed and cells migrated through the membrane to the lower surface were fixed and stained with 0.5% crystal violet for 30 min and quantified by bright-field imaging.

Western Blot Analysis. MCF-7 cells were grown in 100 mm petri dishes and treated with CCL2 (50 ng) and heparin mimetics (50 μg) for half hour. The cells were pelleted and treated with protease inhibitors before treating with lysis buffer containing 150 mM NaCl, 1% NP-40, 0.25% sodium dodecyl sulfate (SDS), 1 mM ethylenediaminetetraacetic acid (EDTA), and 1 mM phenylmethane sulfonyl fluoride (PMSF) in 50 mM Tris-Cl (pH 7.4). After 1 h, the supernatant was collected by centrifugation (14,000 rpm) for 15 min and stored in aliquots. The protein content was quantified using the Bradford method. The protein (35 μg) was loaded for SDS-polyacrylamide gel electrophoresis (10%) and transferred onto a polyvinylidene fluoride (PVDF) membrane. The membrane was incubated for 2 h with specific antibodies corresponding to MAPK. The membranes were incubated with horse radish peroxidase (HRP)-conjugated secondary antibody for 1 h at RT, and visualization was done using an Immobilon Western Chemiluminescent HRP substrate kit (Millipore Corporation, MA, USA) with GAPDH as an internal standard. BioRad's Protein Ladder (Thermo, EU) was used to determine the molecular weights of the protein bands..

■ ASSOCIATED CONTENT

Supporting Information

The Supporting Information is available free of charge at https://pubs.acs.org/doi/10.1021/acs.jmedchem.0c01800.

SPR sensorgrams, primary and secondary antibodies and detection concentrations used on the array, RFUs graphs, FACS analysis histographs, bright-field images of cell invasion assay, Western blot quantification, NMR spectral data, and molecular formula strings and some data (PDF)

SMILES data for compounds (CSV)

https://dx.doi.org/10.1021/acs.jmedchem.0c01800
J. Med. Chem. 2021, 64, 3367−3380

AUTHOR INFORMATION

Corresponding Authors

Vered Padler-Karavani − *Department of Cell Research and Immunology, the Shmunis School of Biomedicine and Cancer Research, the George S. Wise Faculty of Life Sciences, Tel Aviv University, Tel Aviv 69978, Israel;* orcid.org/0000-0002-4761-3571; Email: vkaravani@tauex.tau.ac.il

Raghavendra Kikkeri − *Indian Institute of Science Education and Research, Pune 411008, India;* orcid.org/0000-0002-4451-6338; Email: rkikkeri@iiserpune.ac.in

Authors

Chethan D. Shanthamurthy − *Indian Institute of Science Education and Research, Pune 411008, India*

Shani Leviatan Ben-Arye − *Department of Cell Research and Immunology, the Shmunis School of Biomedicine and Cancer Research, the George S. Wise Faculty of Life Sciences, Tel Aviv University, Tel Aviv 69978, Israel*

Nanjundaswamy Vijendra Kumar − *Indian Institute of Science Education and Research, Pune 411008, India*

Sharon Yehuda − *Department of Cell Research and Immunology, the Shmunis School of Biomedicine and Cancer Research, the George S. Wise Faculty of Life Sciences, Tel Aviv University, Tel Aviv 69978, Israel*

Ron Amon − *Department of Cell Research and Immunology, the Shmunis School of Biomedicine and Cancer Research, the George S. Wise Faculty of Life Sciences, Tel Aviv University, Tel Aviv 69978, Israel*

Robert J. Woods − *Complex Carbohydrate Research Center, University of Georgia, Athens 306062, Georgia, United States;* orcid.org/0000-0002-2400-6293

Complete contact information is available at: https://pubs.acs.org/10.1021/acs.jmedchem.0c01800

Notes

The authors declare no competing financial interest.

ACKNOWLEDGMENTS

Financial support from the IISER, Pune, DBT (grant nos. BT/PR21934/NNT/28/1242/2017, BT/PR34475/MED/15/210/2020), STARS/APR2019/CS/426/FS and SERB/F/9228/2019−2020 are gratefully acknowledged (to R.K.). This work was supported by the Israel Science Foundation (ISF; to V.P.K.). Acknowledgement to Prof. John Gallagher for valuable suggestions and future collaboration.

DEDICATION

This work is dedicated to Prof. J. D. Esko on his contribution to heparan sulfate glycobiology.

ABBREVIATIONS

CAM, ceric ammonium molybdate; $Cu(OTf)_2$, copper(II) trifluoromethanesulfonate; Cy3-SA, Cy3-sterptavidin; DMF, *N*,*N*-dimethylformamide; EDC, *N*-(3-dimethylaminopropyl)-*N*′-ethylcarbodiimide hydrochloride; EDTA, ethylenediaminetetraacetic acid; GAG, glycosaminoglycan; GlcA, D-glucuronic acid; HPLC, high-performance liquid chromatography; HS, heparan sulfate; HSBPs, heparan sulfate binding proteins; IdoA, L-iduronic acid; Lev, levulinoyl; MAPK, mitogen-activated protein kinase; MeOH, methyl alcohol; NHS, *N*-hydroxysuccinimide; NIS, *N*-iodosuccinimide; PBS, phosphate-buffered saline; PBST, phosphate buffered saline with Tween; PMSF, phenylmethane sulfonyl fluoride; PVDF, polyvinylidene fluoride; RFU, relative fluorescent units; RMSD, root-mean-square deviation; SEM, scanning electron microscope; $SO_3{\cdot}Et_3N$, sulfertrioxide triethylamine; SPR, surface plasmon resonance; TEMPO, (2,2,6,6-tetramethylpiperidin-1-yl)oxyl; THF, tetrahydrofuran; TLC, thin layer chromatography; TMSOTf, trimethylsilyl trifluoromethanesulfonate; TNBC, triple negative breast cancer; WST, water soluble tetrazolium

REFERENCES

(1) Luster, A. D. Chemokines-chemotatic cytokines that mediate inflammation. *N. Engl. J. Med.* **1998**, *338*, 436−445.

(2) Charo, I. F.; Ransohoff, R. M. The many roles of chemokines and chemokine receptors in inflammation. *N. Engl. J. Med.* **2006**, *354*, 610−621.

(3) Brylka, L. J.; Schinke, T. Chemokines in physiological and pathological bone remodelling. *Front. Immunol.* **2019**, *10*, 2182.

(4) Schall, T. J.; Proudfoot, A. E. I. Overcoming hurdles in developing successful drugs targeting chemokine receptors. *Nat. Rev. Immunol.* **2011**, *11*, 355−363.

(5) Koenen, R. R.; Weber, C. Therapeutic targeting of chemokine interactions in atherosclerosis. *Nat. Rev. Drug Discovery* **2010**, *9*, 141−153.

(6) Lacotte, S.; Brun, S.; Muller, S.; Dumortier, H. CXCR3, inflammation and autoimmune diseases. *Ann. N.Y. Acad. Sci.* **2009**, *1173*, 310−317.

(7) Fuchs, J. A.; Brunner, C.; Schineis, P.; Hiss, J. A.; Schneider, G. Identification of chemokine ligands by biochemical fragmentation and simulated peptide evolution. *Angew. Chem., Int. Ed.* **2019**, *58*, 7138−7142.

(8) Fernandez, A.; Thompson, E. J.; Pollard, J. W.; Kitamura, T.; Vendrell, M. A fluorescent activatable AND-Gate chemokine CCL2 enables in vivo detection of metastasis-associated macrophages. *Angew. Chem., Int. Ed.* **2019**, *58*, 16894−16898.

(9) Korniejewska, A.; McKnight, A. J.; Johnson, Z.; Watson, M. L.; Ward, S. G. Expression and agonist responsiveness of CXCR3 variants in human T lymphocytes. *Immunology* **2011**, *132*, 503−515.

(10) Raman, D.; Sobolik-Delmaire, T.; Richmond, A. Chemokines in health and disease. *Exp. Cell Res.* **2011**, *317*, 575−589.

(11) van Kasteren, S. I.; Neefjes, J.; Ovaa, H. Creating molecules that modulate immune responses. *Nat. Rev. Chem.* **2018**, *2*, 184−193.

(12) Kitamura, T.; Pollard, J. W. Therapeutic potential of chemokine signal inhibition for metastatic breast cancer. *Pharmacol. Res.* **2015**, *100*, 266−270.

(13) Andrews, S. P.; Cox, R. J. Small molecule CXCR3 antagonists. *J. Med. Chem.* **2016**, *59*, 2894−2917.

(14) De Cleroq, E. The AMD3100 story: the path to the discovery of a stem cell mobilize (Mozobil). *Biochem. Pharmacol.* **2009**, *77*, 1655−1664.

(15) Pierry, C. M. Marviroc: a review of its use in the management of CCR5-tropic HIV-1 infection. *Drugs* **2010**, *70*, 1189−1213.

(16) Lortat-Jacob, H. The molecular basis and functional implications of chemokine interactions with heparan sulfate. *Curr. Opin. Struct. Biol.* **2009**, *19*, 543−548.

(17) Johnson, Z.; Proudfoot, A. E.; Handel, T. M. Interaction of chemokines and glycosaminoglycans: a new twist in the regulation of chemokine function with opportunities for therapeutic intervention. *Cytokine Growth Factor Rev.* **2005**, *16*, 625−636.

(18) Handel, T. M.; Johnson, Z.; Crown, S. E.; Lau, E. K.; Sweeney, M.; Proudfoot, A. E. Regulation of protein function by glycosaminoglycans as exemplified by chemokines. *Annu. Rev. Biochem.* **2005**, *74*, 385−410.

(19) Kufareva, I.; Salanga, C. L.; Handel, T. M. Chemokine and chemokine receptor structure and interactions: implications for therapeutic strategies. *Immunol. Cell Biol.* **2015**, *93*, 372−383.

(20) Xu, D.; Esko, J. D. Demystifying heparan sulfate-protein interactions. *Annu. Rev. Biochem.* **2014**, *83*, 129−157.

(21) Gandhi, N. S.; Mancera, R. L. The structure of glycosaminoglycans and their interactions with proteins. *Chem. Biol. Drug Des.* **2008**, *72*, 455−482.
(22) Proudfoot, A. E. I.; Handel, T. M.; Johnson, Z.; Lau, E. K.; LiWang, P.; Clark-Lewis, I.; Borlat, F.; Wells, T. N. C.; Kosco-Vilbois, M. H. Glycosaminoglycan binding and oligomerization are essential for the in vivo activity of certain chemokines. *Proc. Natl. Acad. Sci. U.S.A.* **2003**, *100*, 1885−1890.
(23) Shi, X.; Zaia, J. Organ-specific heparan sulfate structural phenotypes. *J. Biol. Chem.* **2009**, *284*, 11806−11814.
(24) Feyzi, E.; Saldeen, T.; Larsson, E.; Lindahl, U.; Salmivirta, M. Age-dependent modulation of heparan sulfate structure and function. *J. Biol. Chem.* **1998**, *273*, 13395−13398.
(25) Brickman, Y. G.; Ford, M. D.; Gallagher, J. T.; Nurcombe, V.; Bartlett, P. F.; Turnbull, J. E. Structural modification of fibroblast growth factor-binding heparan sulfate at a determinative stage of neural development. *J. Biol. Chem.* **1998**, *273*, 4350−4359.
(26) Lindahl, U.; Kjellén, L. Pathophysiology of heparan sulfate: many diseases, few drugs. *J. Intern. Med.* **2013**, *273*, 555−571.
(27) Nadanaka, S.; Kitagawa, H. Heparan sulfate biosynthesis and disease. *J. Biochem.* **2008**, *144*, 7−14.
(28) Petitou, M.; van Boeckel, C. A. A. A synthetic antithrombin III binding pentasaccharide is now a drug! What comes next? *Angew. Chem., Int. Ed.* **2004**, *43*, 3118−3133.
(29) Gama, C. I.; Hsieh-Wilson, L. C. Chemical approaches to deciphering the glycosaminoglycan code. *Curr. Opin. Chem. Biol.* **2005**, *9*, 609−619.
(30) de Paz, J. L.; Moseman, E. A.; Noti, C.; Polito, L.; von Andrian, U. H.; Seeberger, P. H. Profiling heparin-chemokine interactions using synthetic tools. *ACS Chem. Biol.* **2007**, *2*, 735−744.
(31) Nonaka, M.; Bao, X.; Matsumura, F.; Götze, S.; Kandasamy, J.; Kononov, A.; Broide, D. H.; Nakayama, J.; Seeberger, P. H.; Fukuda, M. Synthetic di-sulfated iduronic acid attenuates asthmatic response by blocking T-cell recruitment to inflammatory site. *Proc. Natl. Acad. Sci. U.S.A.* **2014**, *111*, 8173−8178.
(32) Lu, W.; Zong, C.; Chopra, P.; Pepi, L. E.; Xu, Y.; Amster, I. J.; Liu, J.; Boons, G.-J. Controlled chemoenzymatic synthesis of heparan sulfate oligosaccharides. *Angew. Chem., Int. Ed.* **2018**, *57*, 5340−5344.
(33) de Paz, J. L.; Noti, C.; Seeberger, P. H. Microarrays of synthetic heparin oligosaccharides. *J. Am. Chem. Soc.* **2006**, *128*, 2766−2767.
(34) Yoshida, K.; Yang, B.; Yang, W.; Zhang, Z.; Zhang, J.; Huang, X. Chemical synthesis of syndecan-3 glycopeptides bearing two heparan sulfate glycan chains. *Angew. Chem., Int. Ed.* **2014**, *53*, 9051−9058.
(35) Sankaranarayanan, N. V.; Strebel, T. R.; Boothello, R. S.; Sheerin, K.; Raghuraman, A.; Sallas, F.; Mosier, P. D.; Watermeyer, N. D.; Oscarson, S.; Desai, U. R. A hexasaccharide containing rare 2-O-sulfate-glucuronic acid residues selectively activates heparin cofactor II. *Angew. Chem., Int. Ed.* **2017**, *56*, 2312−2317.
(36) Arungundram, S.; Al-Mafraji, K.; Asong, J.; Leach, F. E.; Amster, I. J.; Venot, A.; Turnbull, J. E.; Boons, G.-J. Modular synthesis of heparan sulfate oligosaccharides for structure-activity relationship studies. *J. Am. Chem. Soc.* **2009**, *131*, 17394−17405.
(37) Zong, C.; Venot, A.; Li, X.; Lu, W.; Xiao, W.; Wilkes, J.-S. L.; Salanga, C. L.; Handel, T. M.; Wang, L.; Wolfert, M. A.; Boons, G.-J. Heparan sulfate microarray reveals that heparan sulfate-protein binding exhibits different ligand requirements. *J. Am. Chem. Soc.* **2017**, *139*, 9534−9543.
(38) Zhang, X.; Lin, L.; Huang, H.; Linhardt, R. J. Chemoenzymatic synthesis of glycosaminoglycans. *Acc. Chem. Res.* **2020**, *53*, 335−346.
(39) Jayson, G. C.; Hansen, S. U.; Miller, G. J.; Cole, C. L.; Rushton, G.; Avizienyte, E.; Gardiner, J. M. Synthetic heparan sulfate dodecasaccharides reveal single sulfation site interconverts CXCL8 and CXCL12 chemokine biology. *Chem. Commun.* **2015**, *51*, 13846−13849.
(40) Sepuru, K. M.; Nagarajan, B.; Desai, U. R.; Rajarathnam, K. Molecular basis of chemokine CXCL5-glycosaminoglycan interactions. *J. Biol. Chem.* **2016**, *291*, 20539−20550.
(41) Sepuru, K. M.; Nagarajan, B.; Desai, U. R.; Rajarathnam, K. Structural basis, stoichiometry, and thermodynamics of binding of the chemokines KC and MIPs to the glycosaminoglycan heparin. *J. Biol. Chem.* **2018**, *293*, 17817−17828.
(42) McCanney, G. A.; McGrath, M. A.; Otto, T. D.; Burchmore, R.; Yates, E. A.; Bavington, C. D.; Willison, H. J.; Turnbull, J. E.; Barnett, S. C. Low sulfated heparins target multiple proteins for central nervous system repair. *Glia* **2019**, *67*, 668−687.
(43) Griffin, M. E.; Hsieh-Wilson, L. C. Synthetic probes of glycosaminoglycan function. *Curr. Opin. Chem. Biol.* **2013**, *17*, 1014−1022.
(44) Ziarek, J. J.; Veldkamp, C. T.; Zhang, F.; Murray, N. J.; Kartz, G. A.; Liang, X.; Su, J.; Baker, J. E.; Linhardt, R. J.; Volkman, B. F. Heparin oligosaccharides inhibit chemokine (CXC motif) ligand 12 (CXCL12) cardioprotection by binding orthogonal to the dimerization interface, promoting oligomerization, and competing with the chemokine (CXC motif) receptor 4 (CXCR4) N terminus. *J. Biol. Chem.* **2013**, *288*, 737−746.
(45) Peterson, F. C.; Elgin, E. S.; Nelson, T. J.; Zhang, F.; Hoeger, T. J.; Linhardt, R. J.; Volkman, B. F. Identification and characterization of a glycosaminoglycan recognition element of the C chemokine lymphotactin. *J. Biol. Chem.* **2004**, *279*, 12598−12604.
(46) Sheng, G. J.; Oh, Y. I.; Chang, S.-K.; Hsieh-Wilson, L. C. Tunable heparan sulfate mimetics for modulating chemokine activity. *J. Am. Chem. Soc.* **2013**, *135*, 10898−10901.
(47) Pawar, N. J.; Wang, L.; Higo, T.; Bhattacharya, C.; Kancharla, P. K.; Zhang, F.; Baryal, K.; Huo, C. X.; Liu, J.; Linhardt, R. J.; Huang, X.; Hsieh-Wilson, L. C. Expedient synthesis of core disaccharide building blocks from natural polysaccharides for heparan sulfate oligosaccharide assembly. *Angew. Chem., Int. Ed.* **2019**, *58*, 18577−18583.
(48) Bemdemsky, V.; Yang, Y.; Brennen, T. V. Immunomodulatory activities of the heparan sulfate mimetic PG545. *Adv. Exp. Med. Biol.* **2020**, *1221*, 461−470.
(49) Chhabra, M.; Ferro, V. PI-88 and related heparan sulfate mimetics. *Adv. Exp. Med. Biol.* **2020**, *1221*, 473−491.
(50) Shanthamurthy, C. D.; Kikkeri, R. Linear synthesis of de novo oligo-iduronic acid. *Eur. J. Org. Chem.* **2019**, *2019*, 2950−2953.
(51) Deshmane, S. L.; Kremlev, S.; Amini, S.; Sawaya, B. E. Monocyte chemoattractant protein-1 (MCP-1): An overview. *J. Interferon Cytokine Res.* **2009**, *29*, 313−326.
(52) Padler-Karavani, V.; Song, X.; Yu, H.; Hurtado-Ziola, N.; Huang, S.; Muthana, S.; Chokhawala, H. A.; Cheng, J.; Verhagen, A.; Langereis, M. A.; Kleene, R.; Schachner, M.; de Groot, R. J.; Lasanajak, Y.; Matsuda, H.; Schwab, R.; Chen, X.; Smith, D. F.; Cummings, R. D.; Varki, A. Cross-comparision of protein recognition of sialic acid diversity on two novel sialoglycan microarrays. *J. Biol. Chem.* **2012**, *287*, 22593−22608.
(53) Ben-Arye, S. V.; Yu, H.; Chen, X.; Padler-Karavani, V. Profiling anti-neu5Gc IgG in human sera with a sialoglycan microarray assay. *J. Visualized Exp.* **2017**, *125*, 56094.
(54) Haasnoot, C. A. G.; de Gelder, R.; Kooijman, H.; Kellenbach, E. R. The conformation of the idopyranose ring revisited: How subtle O-substitutent induced changes can be deduced from vicinal 1H-NMR coupling constants. *Carbohydr. Res.* **2020**, *496*, 108052.
(55) Miller, M.; Mayo, K. Chemokines from a structural perspective. *Int. J. Mol. Sci.* **2017**, *18*, 2088.
(56) Singh, A.; Kett, W. C.; Severin, I. C.; Agyekum, I.; Duan, J.; Amster, I. J.; Proudfoot, A. E. I.; Coombe, D. R.; Woods, R. J. The interaction of heparin tetrasaccharides with chemokine CCL5 is modulated by sulfation pattern and pH. *J. Biol. Chem.* **2015**, *290*, 15421−15436.
(57) Arimont, M.; Sun, S.-L.; Leurs, R.; Smit, M.; De Esch, I. J. P.; de Graaf, C. Structural analysis of chemokine receptor−ligand interactions. *J. Med. Chem.* **2017**, *60*, 4735−4779.
(58) Lu, Y.; Cai, Z.; Xiao, G.; Liu, Y.; Keller, E. T.; Yao, Z.; Zhang, J. CCR2 expression correlates with prostate cancer progression. *J. Cell. Biochem.* **2007**, *101*, 676−685.

https://dx.doi.org/10.1021/acs.jmedchem.0c01800
J. Med. Chem. 2021, 64, 3367−3380

(59) Dutta, P.; Sarkissyan, M.; Paico, K.; Wu, Y.; Vadgama, J. V. MCP-1 is overexpressed in triple-negative breast cancers and drives cancer invasiveness and metastasis. *Breast Cancer Res. Treat.* **2018**, *170*, 477−486.
(60) Sangabathuni, S.; Murthy, R. V.; Gade, M.; Bavireddi, H.; Toraskar, S.; Sonar, M. V.; Ganesh, K. N.; Kikkeri, R. Modeling glycocollagen conjugates using a host guest strategy to alter phenotypic cell migration and in vivo wound healing. *ACS Nano* **2017**, *11*, 11969−11977.
(61) Pettersen, E. F.; Goddard, T. D.; Huang, C. C.; Couch, G. S.; Greenblatt, D. M.; Meng, E. C.; Ferrin, T. E. UCSF Chimera—a visualization system for exploratory research and analysis. *J. Comput. Chem.* **2004**, *25*, 1605−1612.

https://dx.doi.org/10.1021/acs.jmedchem.0c01800
J. Med. Chem. 2021, 64, 3367−3380